A. Einstein: "**Only the theory decides what we will manage to watch!**"

11 апреля, 2017
Москва

Нужно ли применять персонифицированный подход к лечению амилоидозов?

Oxana V. Galzitskaya

The mechanism underlying amyloid polymorphism is opened for Alzheimer's disease Amyloid-β peptide

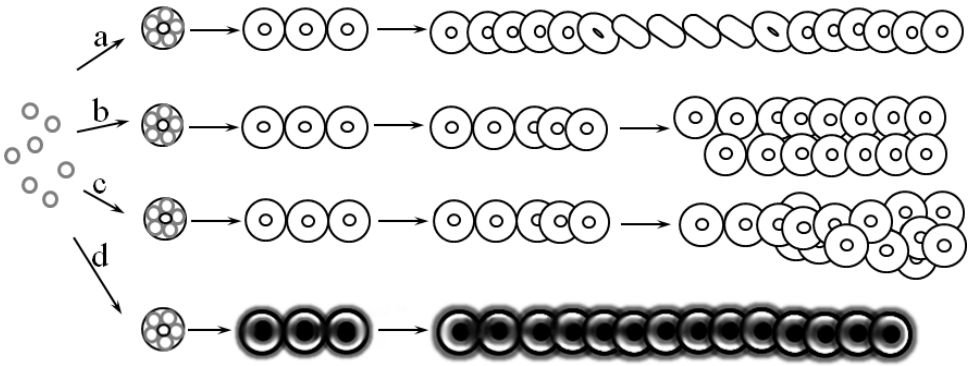

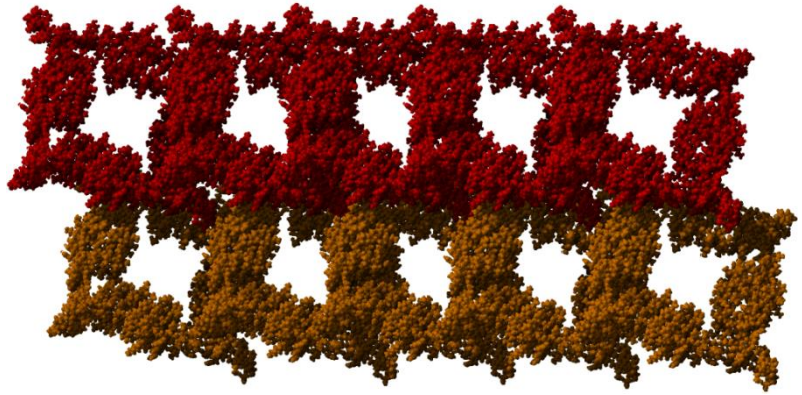

Institute of Protein Research, Russian Academy of Sciences,
4 Institutskaya str., Pushchino, Moscow Region, 142290, Russia

Разнообразие амилоидных фибрилл при болезни Альцгеймера

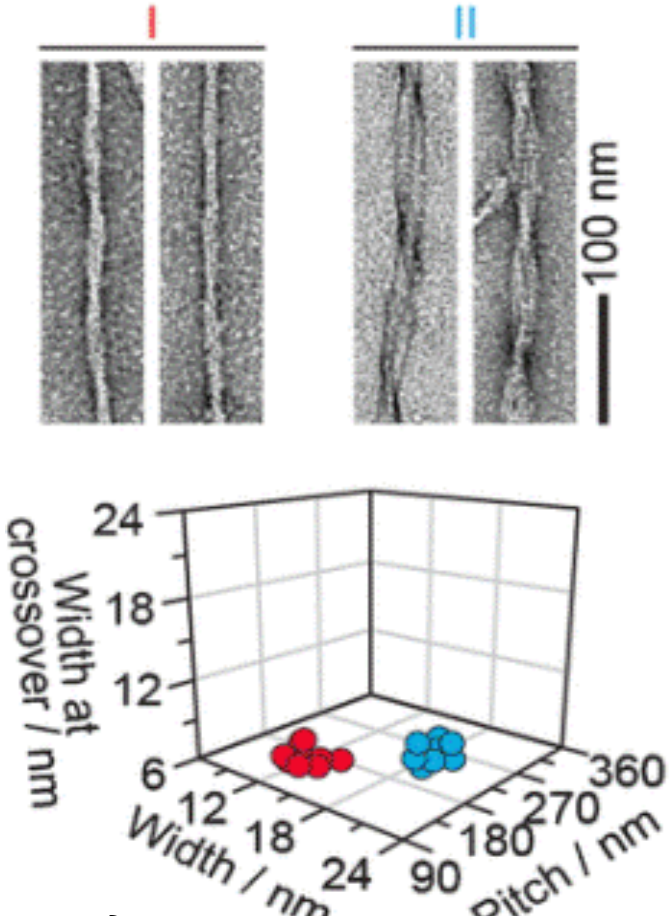

Свидетельство уникального структурного разнообразия амилоидных фибрилл в тканях человека и животных. (Рисунок из Angew. Chem. Int. Ed., 2016, DOI: 10.1002/anie.201511524)

В лаборатории уже было показано, что подобные агрегаты могут различаться морфологией – обладать различной длиной, толщиной и строением региона, в котором они переплетаются, однако до недавнего момента не было понятно, характерно ли такое различие морфологий для обычной биологической ткани. Группа исследователей, работающих под руководством Маркуса Фэндриха (Marcus Fändrich) из Университета Ульма, изучила экстракты из тканей животных и людей, страдающих различными формами амилоидоза, и показала, что и в живой ткани морфология белковых фибрилл различается. Результаты исследования могут оказаться полезными для разработки различных типов лечения амилоидозов.

Structural variation in amyloid-β fibrils from Alzheimer's disease clinical subtypes

2 | NATURE | VOL 000 | 00 MONTH 2016

LETTER RESEARCH

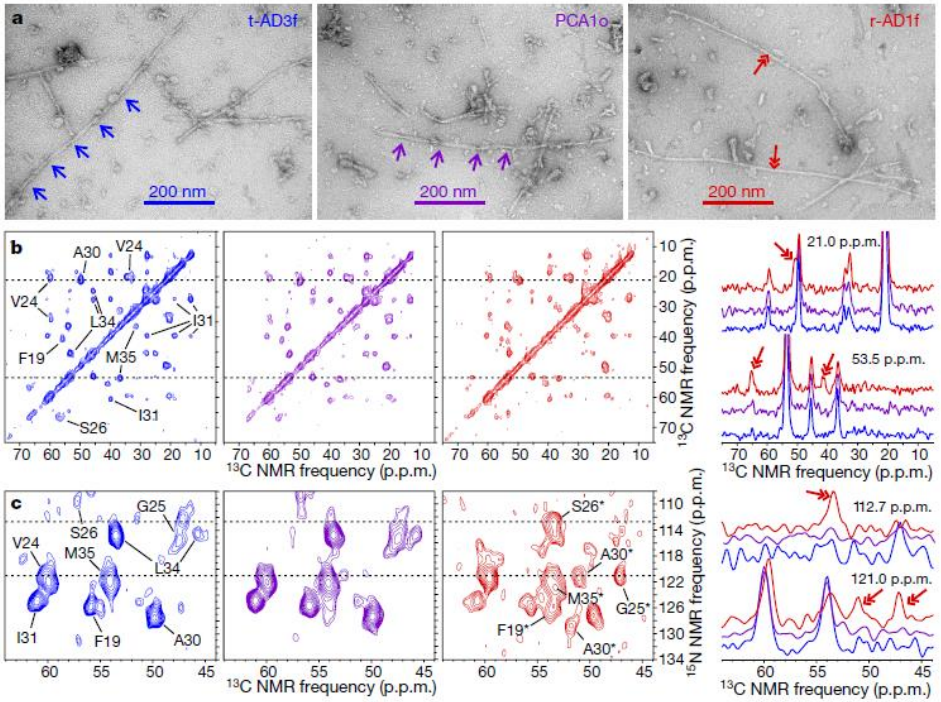

Figure 1 | Representative TEM images and 2D ssNMR spectra of brain-seeded Aβ40 fibrils. **a**, Images of negatively-stained fibrils derived from t-AD3f, PCA1o, and r-AD1f tissue, recorded 4 h after initiation of seeded fibril growth (representative of 37 fibril samples). Single-headed arrows indicate the periodic modulation of apparent fibril width in a common Aβ40 fibril morphology. Double-headed arrows indicate an additional morphology. **b**, Aliphatic regions of 2D ^{13}C–^{13}C spectra of the same samples (colour-coded as in **a**), with assignments of cross-peak signals to isotopically labelled residues shown in the 2D spectrum of t-AD3f fibrils. Aβ40 was uniformly ^{15}N–^{13}C-labelled at residues F19, V24, G25, S26, A30, I31, L34 and M35. Contour levels increase by successive factors of 1.5. Shown on the right are 1D slices at 21.0 p.p.m. and 53.5 p.p.m., with double-headed arrows indicating signals that arise from the less common fibril structures. **c**, The 2D ^{15}N–^{13}C spectra of the same samples, with assignments of the predominant cross-peak signals shown in the 2D spectrum of t-AD3f fibrils and assignments of additional signals (with asterisks) shown in the 2D spectrum of r-AD1f fibrils. Contour levels increase by successive factors of 1.3. Shown on the right are 1D slices at 112.7 p.p.m. and 121.0 p.p.m., with double-headed arrows indicating signals that arise from the less common fibril structures.

Number of articles devoted to studying of different fragments of Aβ peptide from the PubMed (of December 2015)

Dovidchenko et al., J Struct Biol. 2016 Jun;194(3):404-14.

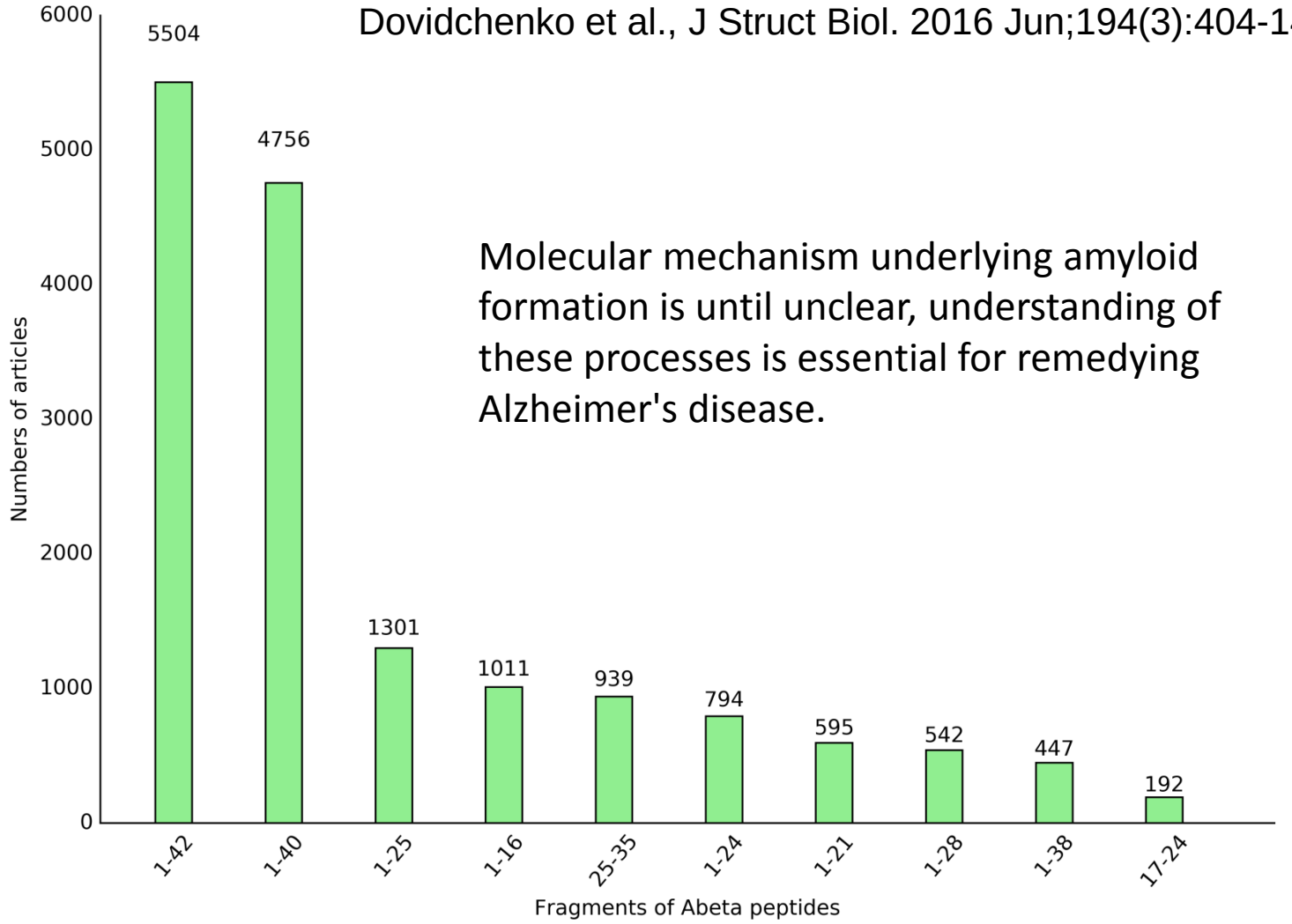

Molecular mechanism underlying amyloid formation is until unclear, understanding of these processes is essential for remedying Alzheimer's disease.

Aβ-peptide forms amyloid fibrils

Aβ-peptide:

- General component of amyloid deposits at Alzheimer's disease;
- Forms polymorphic fibrils;
- Different mechanisms of amyloid formation were described.

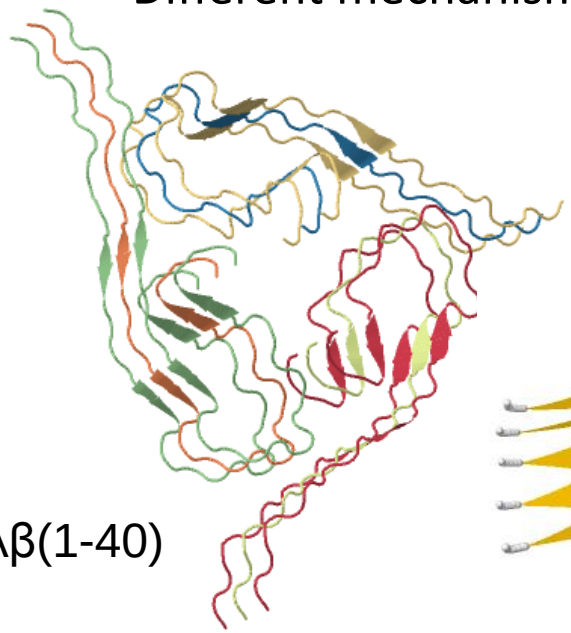

Aβ(1-40)

Paravastu et al.(2008)

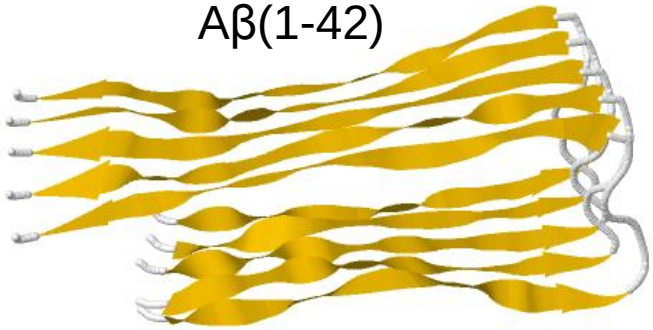

Aβ(1-42)

Luhrs et al.(2005)

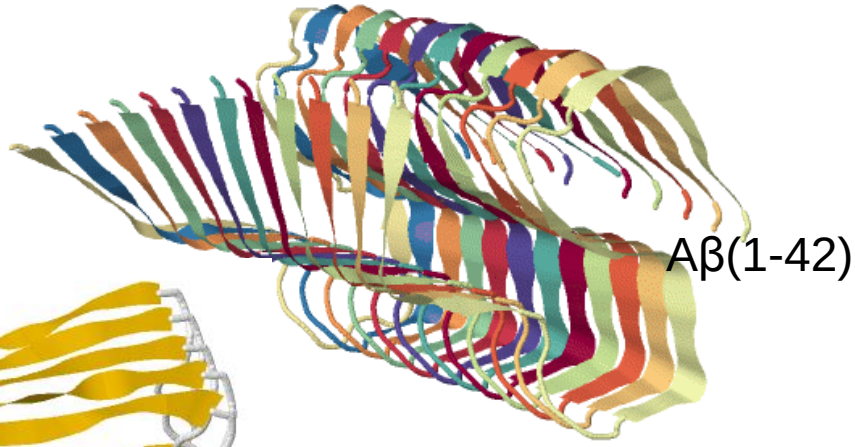

Aβ(1-42)

Xiao et al. (2015)

DETERMINATION OF Aβ-PEPTIDE REGIONS, INCLUDING IN THE AMYLOID FIBRILS, IS IMPORTANT FOR STUDYING MECHANISM OF AMYLOID FORMATION

There is no consistent model describing the molecular mechanism of Aβ amyloid formation

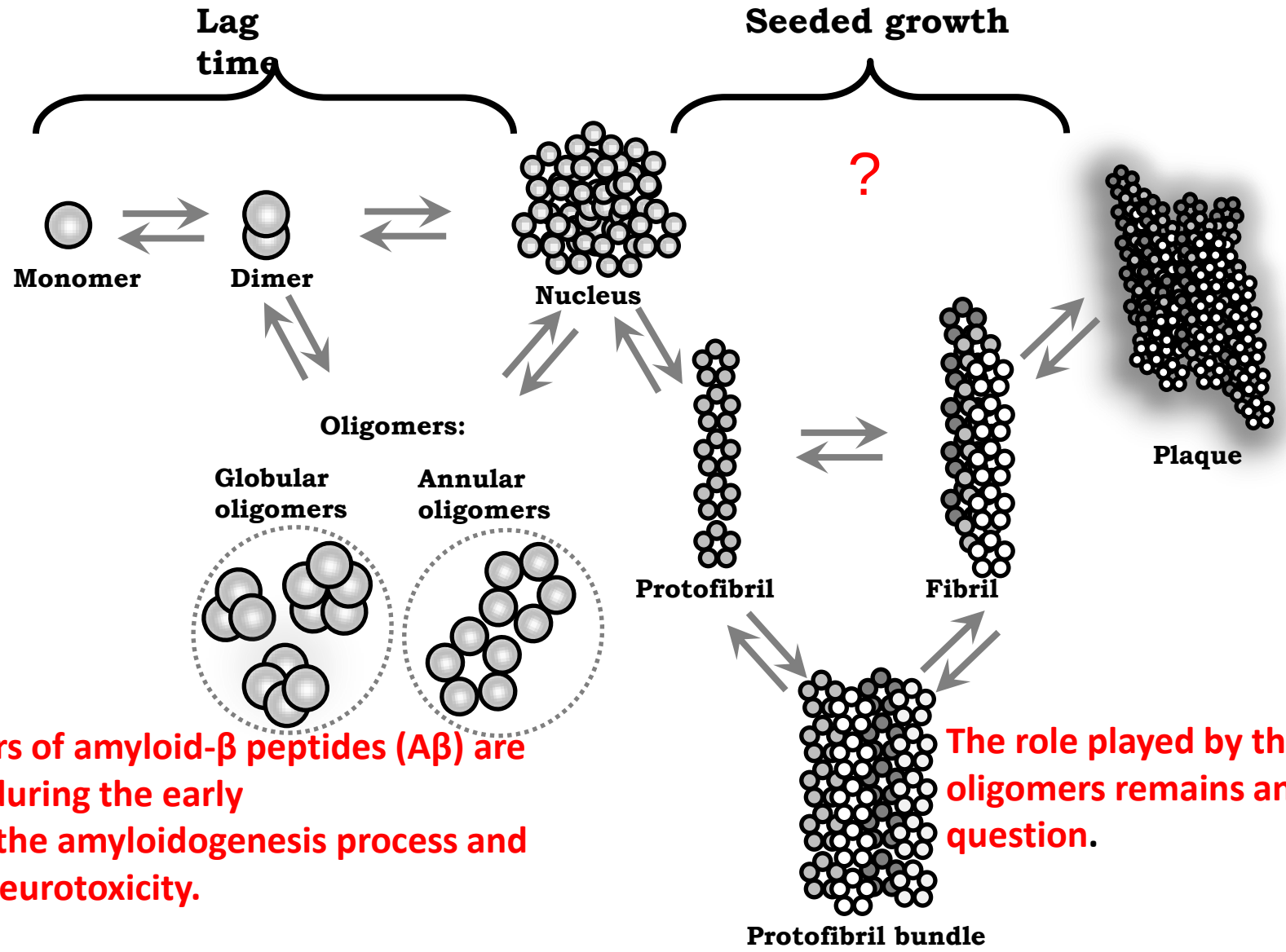

Oligomers of amyloid-β peptides (Aβ) are formed during the early stage of the amyloidogenesis process and exhibit neurotoxicity.

The role played by these oligomers remains an open question.

Schematic mechanism for dihexamer formation

Amyloid β-Protein Oligomerization and the Importance of Tetramers and Dodecamers in the Aetiology of Alzheimer's Disease, Nature chemistry, Berstein et al., 2009, 1(4):326-31

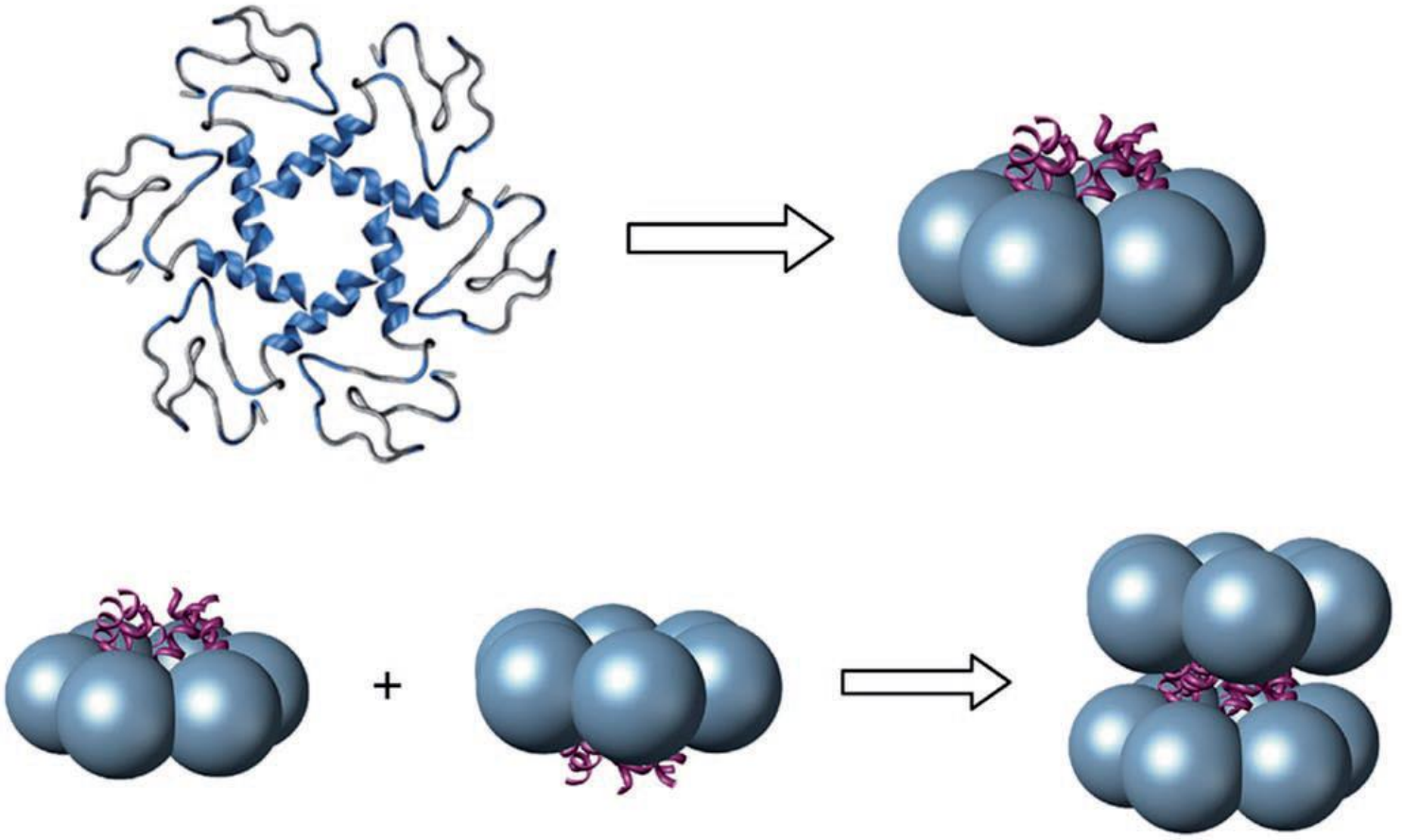

The dodecamer is the terminal species observed in the experiment.

Docking of hexamer units into protofibrils

Lendel et al., Angew. Chem. Int. Ed. 2014, 53, 12756

"It is possible that barrel models with other stoichiometries are also consistent with our NMR data".

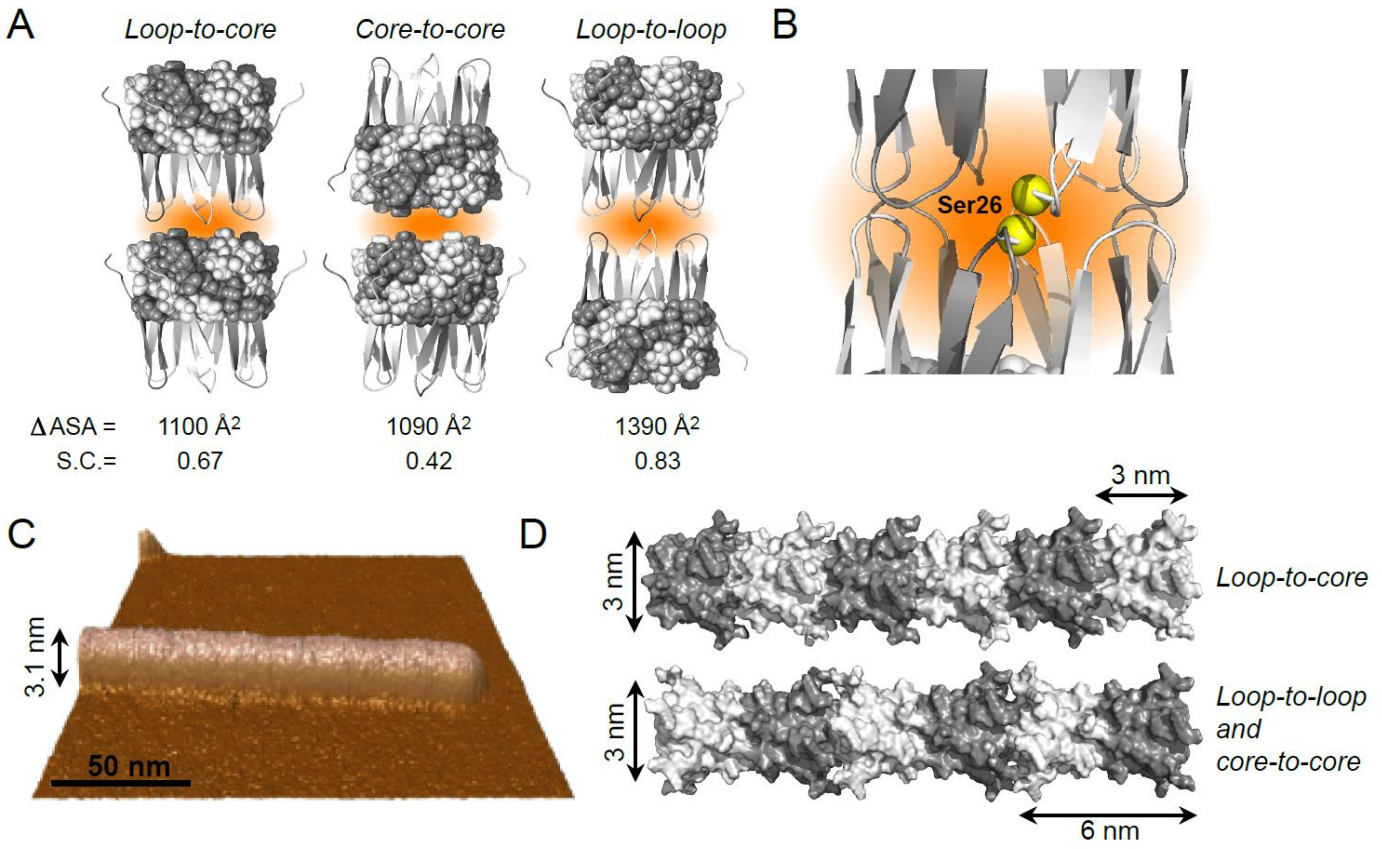

The correlation of secondary shifts in the C-terminal fragment is clear and suggests that the backbone conformation of residues 31-42 in Aβ42CC (Cys21 and Cys30) protofibrils is present already in Aβ42 oligomers that have not yet formed protofibrils.

Dodecamers of Aβ42 Seed Fibril Formation

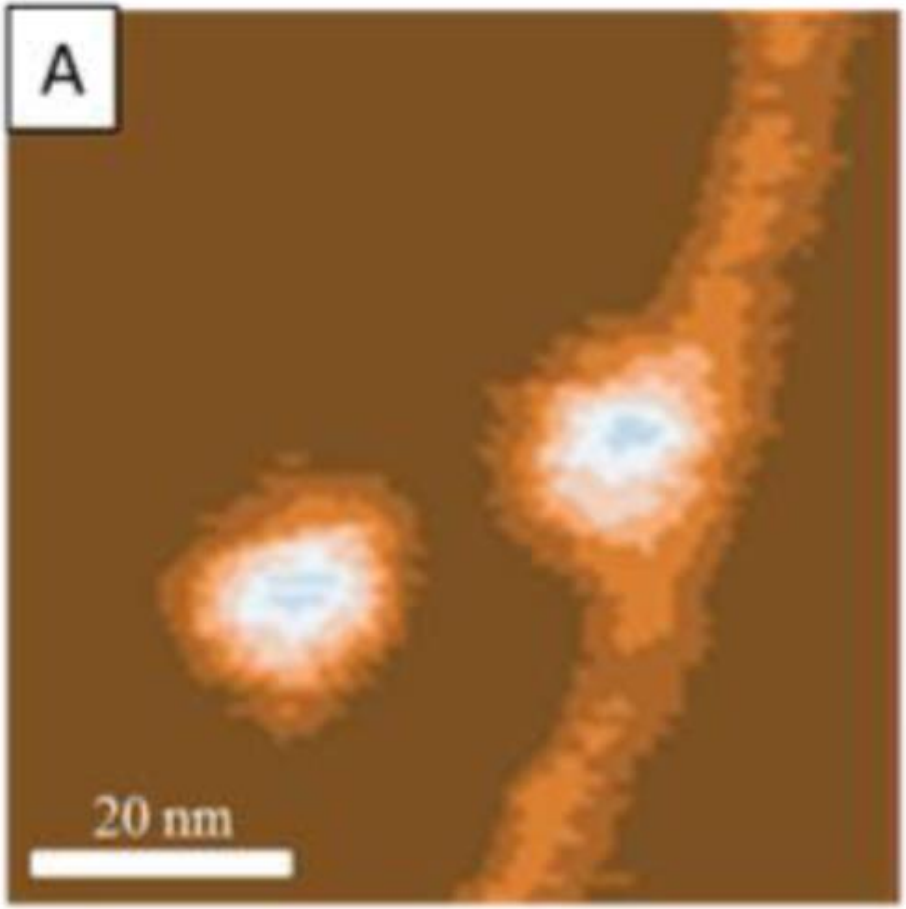

Topographic image of Aβ42 cast from a 1 μM solution after 10 min of incubation showing the interaction between dodecamers and extended preprotofibrils.

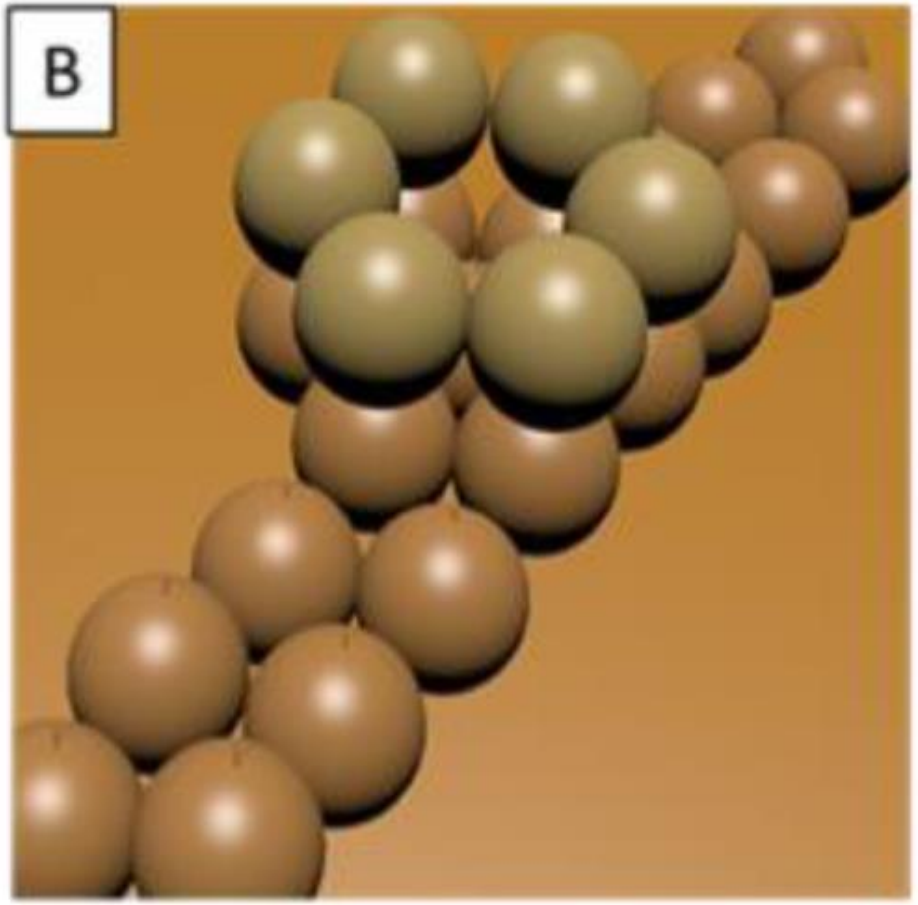

Schematic cartoon of this growth mechanism. (Economou et al., 2016, JACS, 138(6):1772)

Strain-specific Fibril Propagation by an Aβ Dodecamer

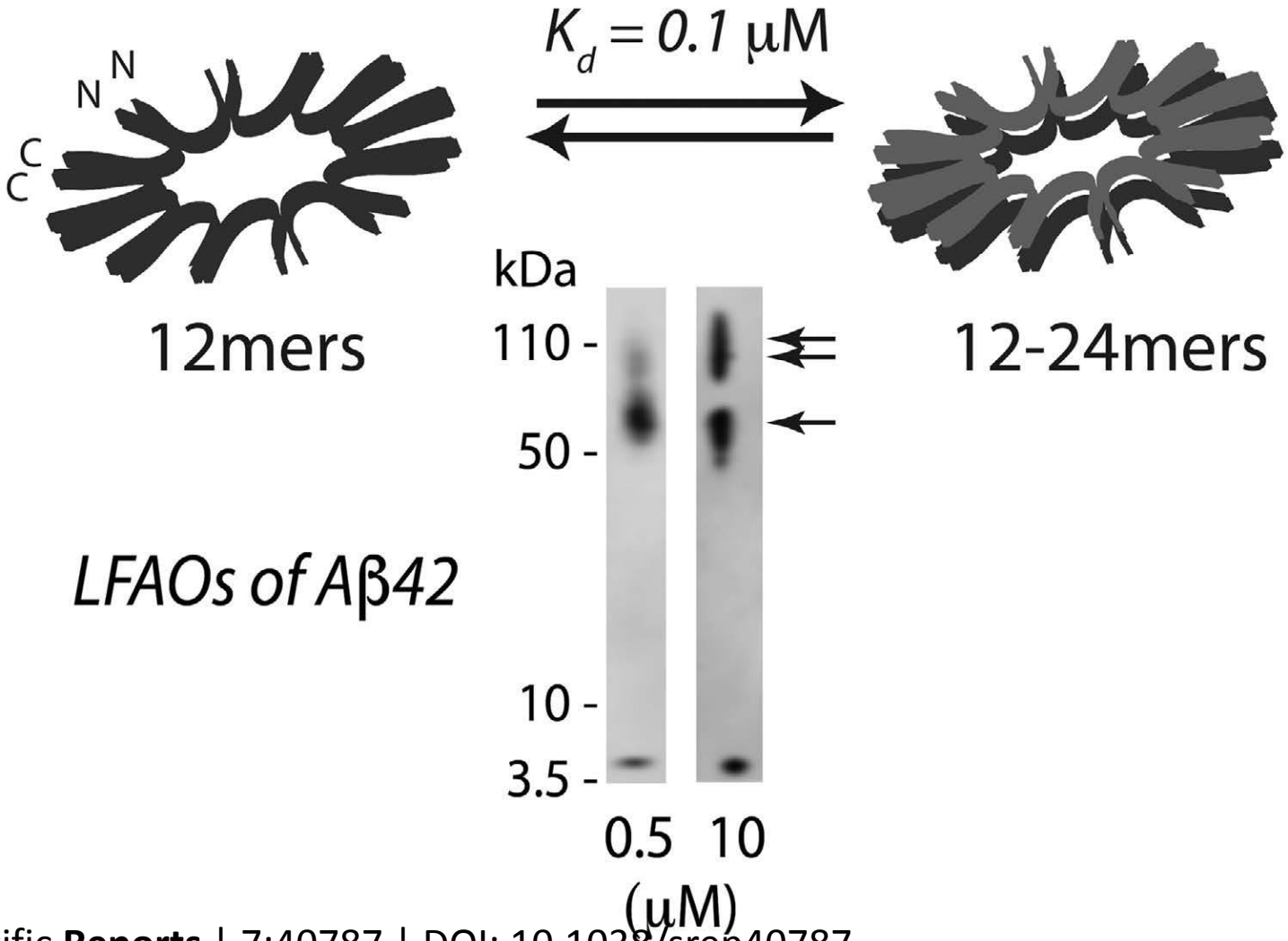

Scientific **Reports** | 7:40787 | DOI: 10.1038/srep40787

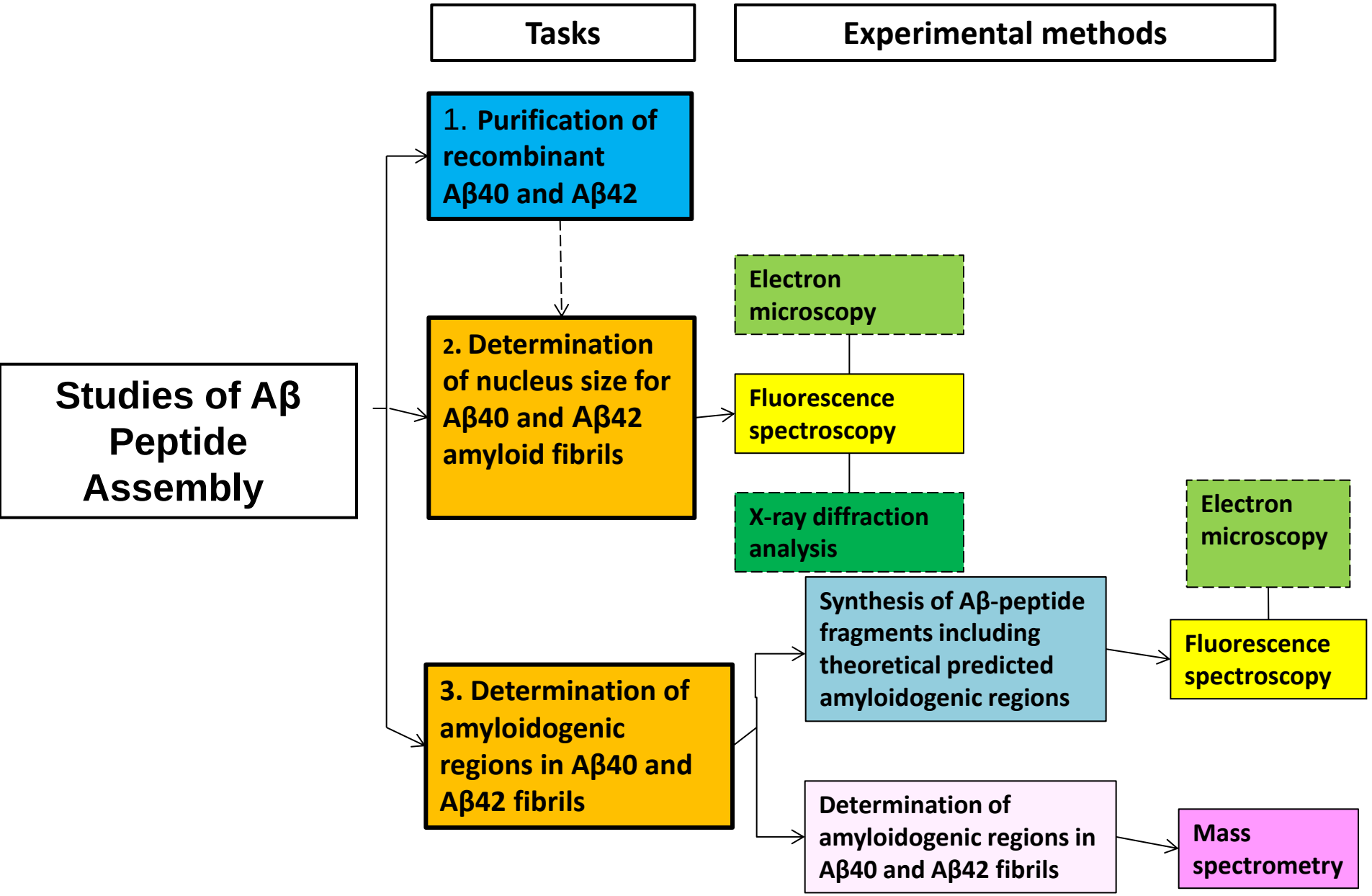
Tasks
Experimental methods
Studies of Aβ Peptide Assembly
1. Purification of recombinant Aβ40 and Aβ42
2. Determination of nucleus size for Aβ40 and Aβ42 amyloid fibrils
3. Determination of amyloidogenic regions in Aβ40 and Aβ42 fibrils
Electron microscopy
Fluorescence spectroscopy
X-ray diffraction analysis
Synthesis of Aβ-peptide fragments including theoretical predicted amyloidogenic regions
Electron microscopy
Fluorescence spectroscopy
Determination of amyloidogenic regions in Aβ40 and Aβ42 fibrils
Mass spectrometry

The question about the size of nuclei of protofibrils formed by different proteins and peptides is yet open and debatable because of the absence of solid knowledge of underlying mechanisms of amyloid formation.

The most unstable state

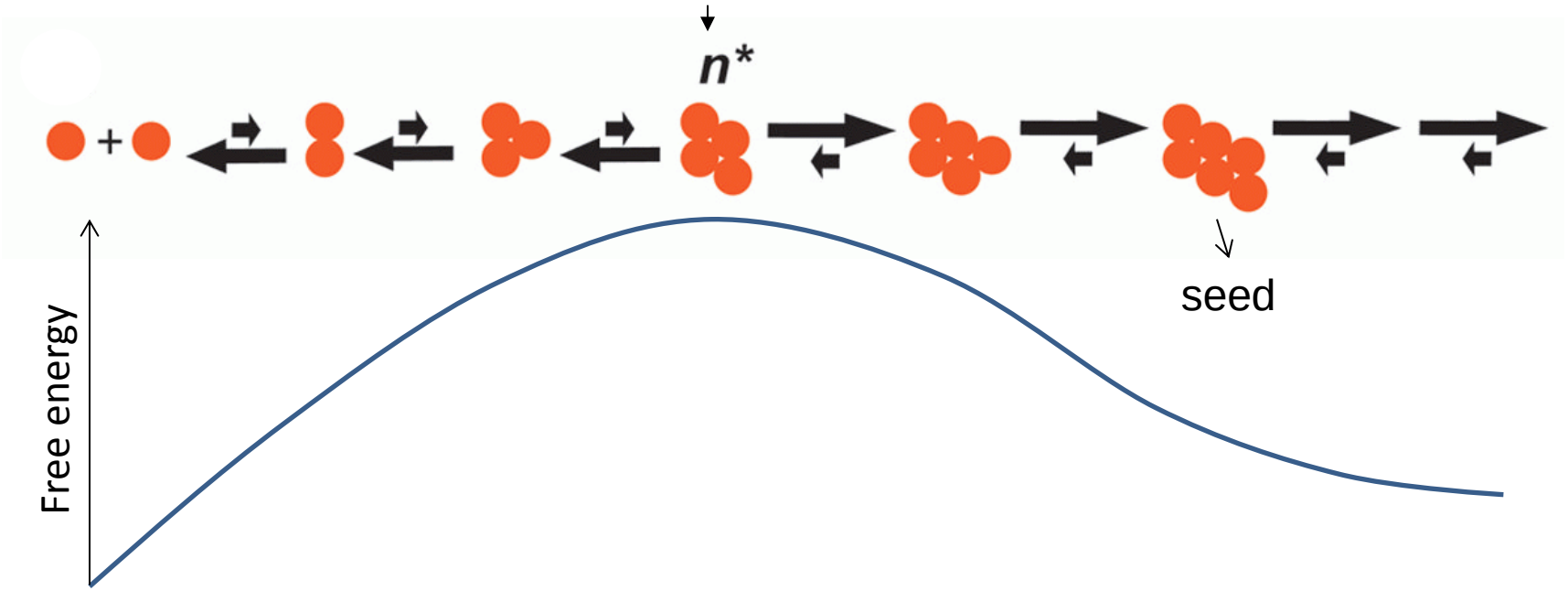

At the nucleation mechanism the formation of protofibrils begins with thermodynamically unfavorable steps, which produces a "critical nucleus" of n* monomers.

Kinetic scenario 1: Linear growth of fibrils from the ends

Oosawa et al., J. Polym. Sci. (1959) 37:323

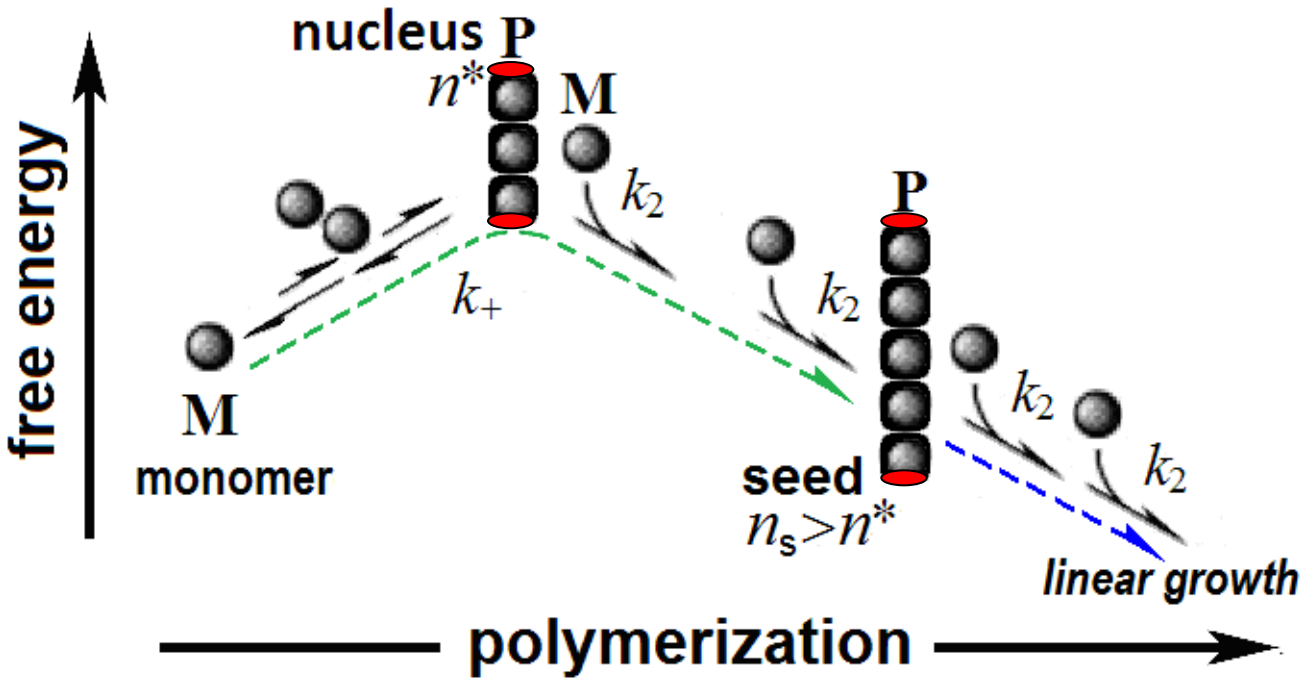

$$n_s \mathbf{M} \xrightarrow[k_+]{} \mathbf{P}_{n_s} \quad \Rightarrow \quad \frac{d[\mathrm{P}]}{dt} = 2k_+[\mathrm{M}]^{n^*}$$

$$\mathbf{P} + \mathbf{M} \xrightarrow[2\_\mathrm{ends}\times k_2]{} \mathbf{P} \quad \Rightarrow \quad \frac{d[\mathrm{M}]}{dt} \approx -k_2[\mathrm{P}][\mathrm{M}]$$

→ strict **analytical** solution for the whole process

Kinetic scenarios 2, 3, 4: Exponential growth of fibrils

leads to a large relative duration L_{rel} of the lag-period

Exponential multiplication of the sticky points

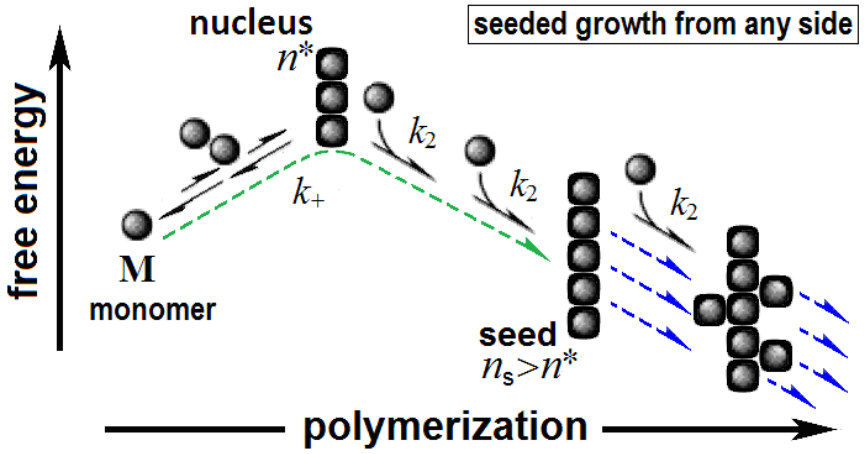

Growth from the surface

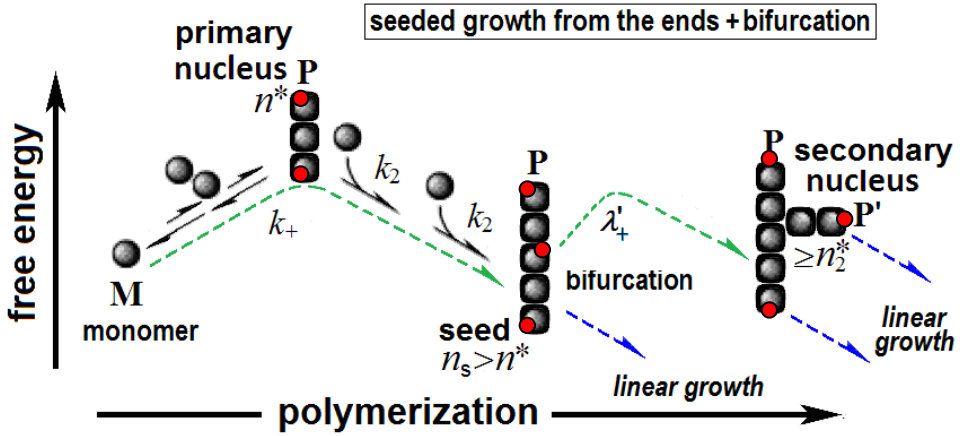

Fibril ends multiplication by branching

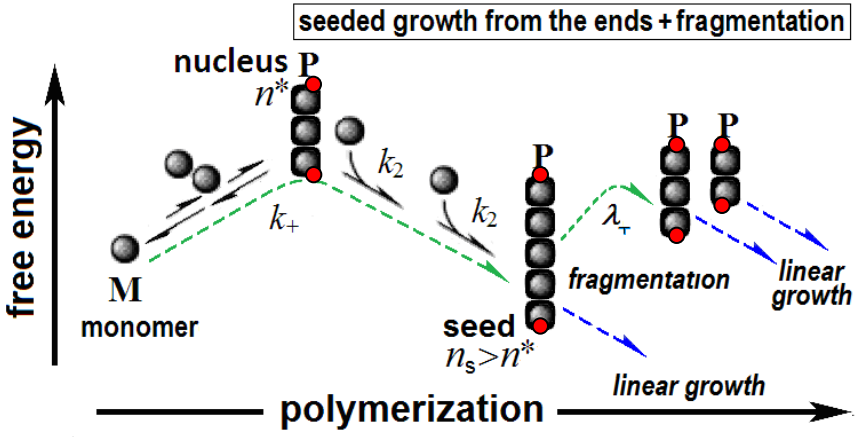

Fibril multiplication by fragmentation

"Secondary (heterogeneous) nucleation":

Ferrone (1999) Methods Enzymol. 309:256;

Dovidchenko et al., 2014, *J. Phys. Chem. B* **118**, 1189–1197

The obtained analytical solution allows us to determine the size of the **primary and secondary nuclei** from the experimentally obtained concentration dependences of the time of growth and the ratio of the lag time duration to the time of growth of amyloid protofibrils.

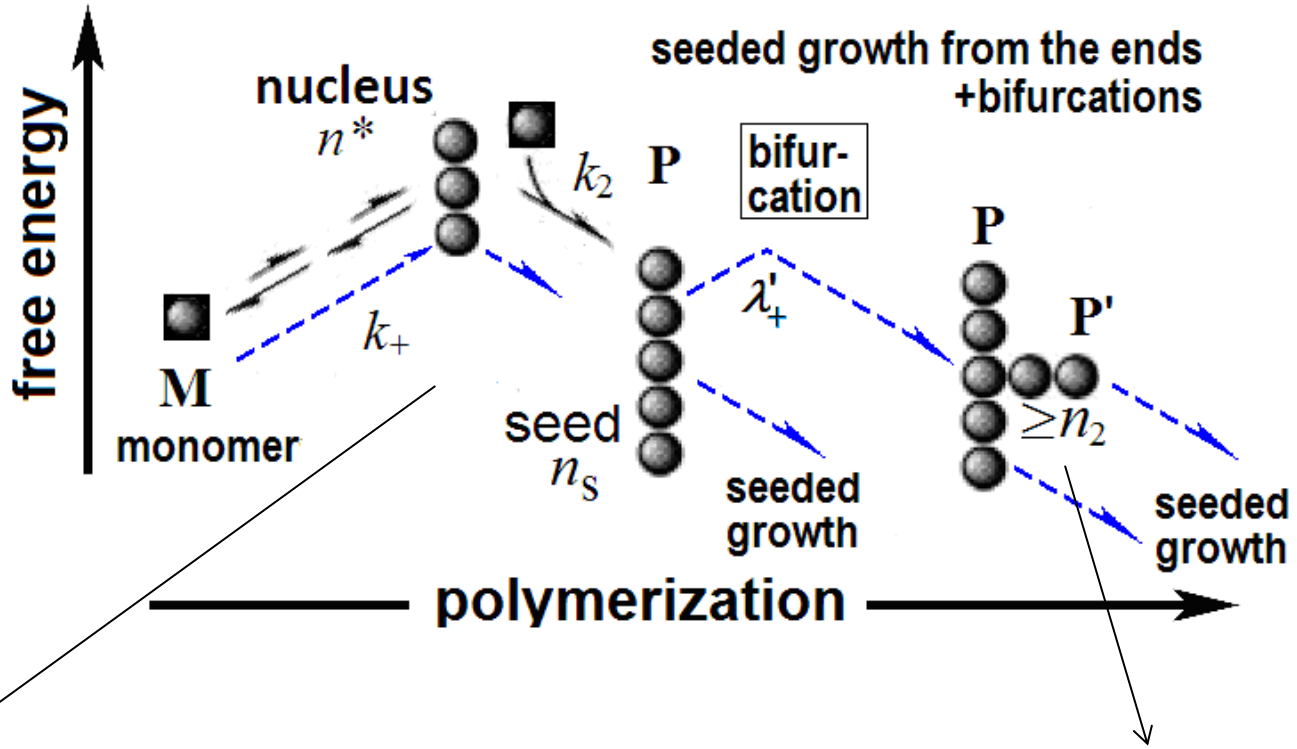

The primary nucleus

$$n^* = 1 + n_2 - \frac{d(\mathrm{L_{rel}})}{d(\ln[\mathrm{M}_\Sigma])}$$

The secondary nucleus

$$n_2 = -1 - 2\frac{d(\ln \mathrm{T}_2)}{d(\ln[\mathrm{M}_\Sigma])}$$

Dovidchenko et al., 2014, *J. Phys. Chem. B* **118**, 1189–1197

Meisl et al., 2014, *Proc Natl Acad Sci U S A* 111(26): 9384

Cohen et al., 2013, *Proc Natl Acad Sci U S A* 110(24): 9758

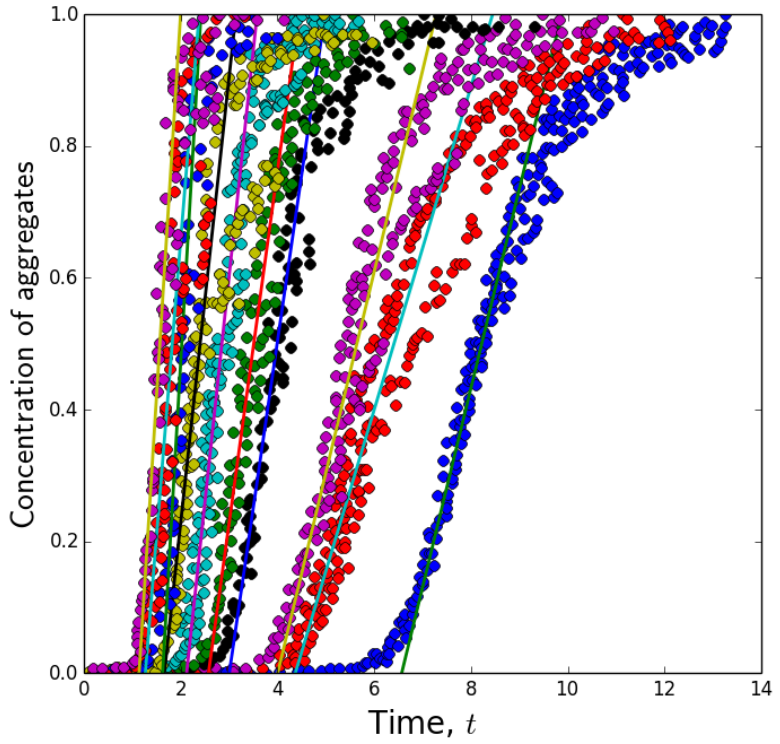

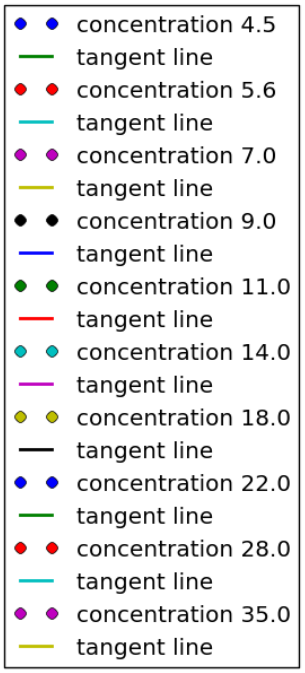

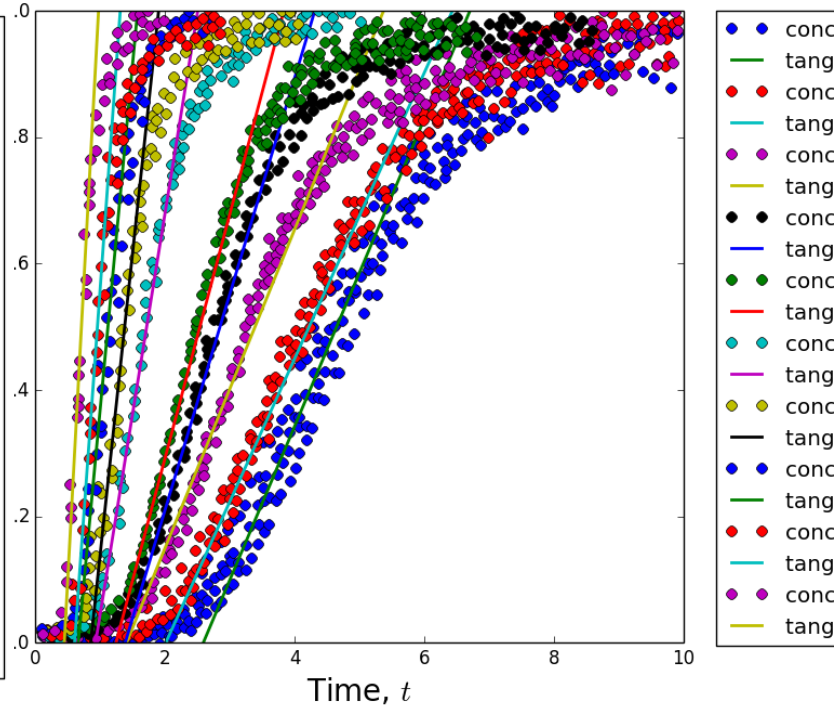

for Aβ40

for Aβ42

Formation of oligomer structures through the nucleus formation (#) for (a) Aβ40 and (b) Aβ42

Aβ40 , n1=2

Aβ42, n1=3

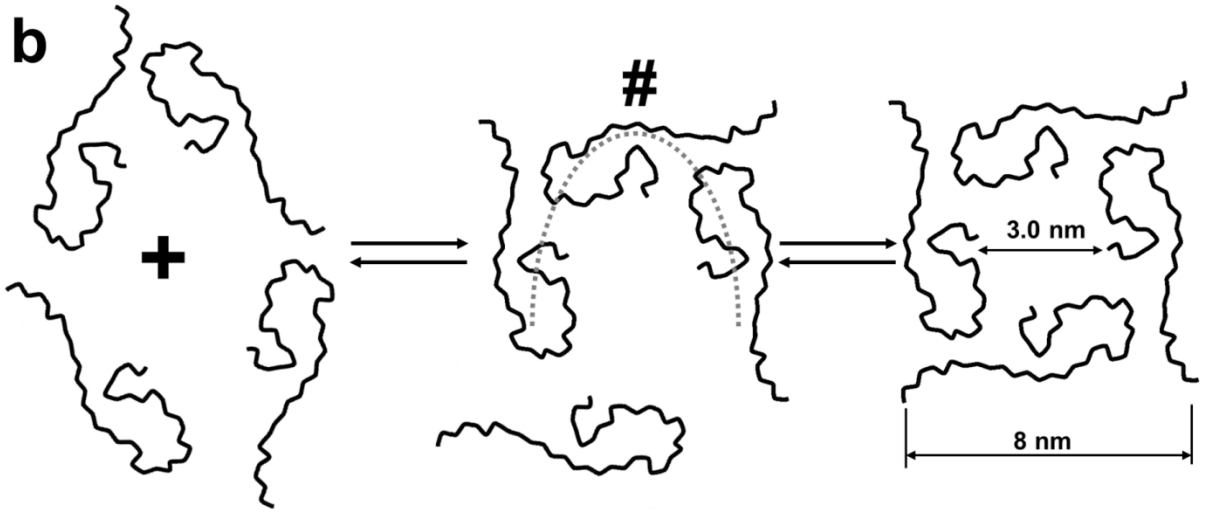

Dovidchenko et al., J Struct Biol. 2016 Jun;194(3):404-14.

Formation of oligomer structures through the nucleus formation (#) for (A) Aβ40 and (B) Aβ42

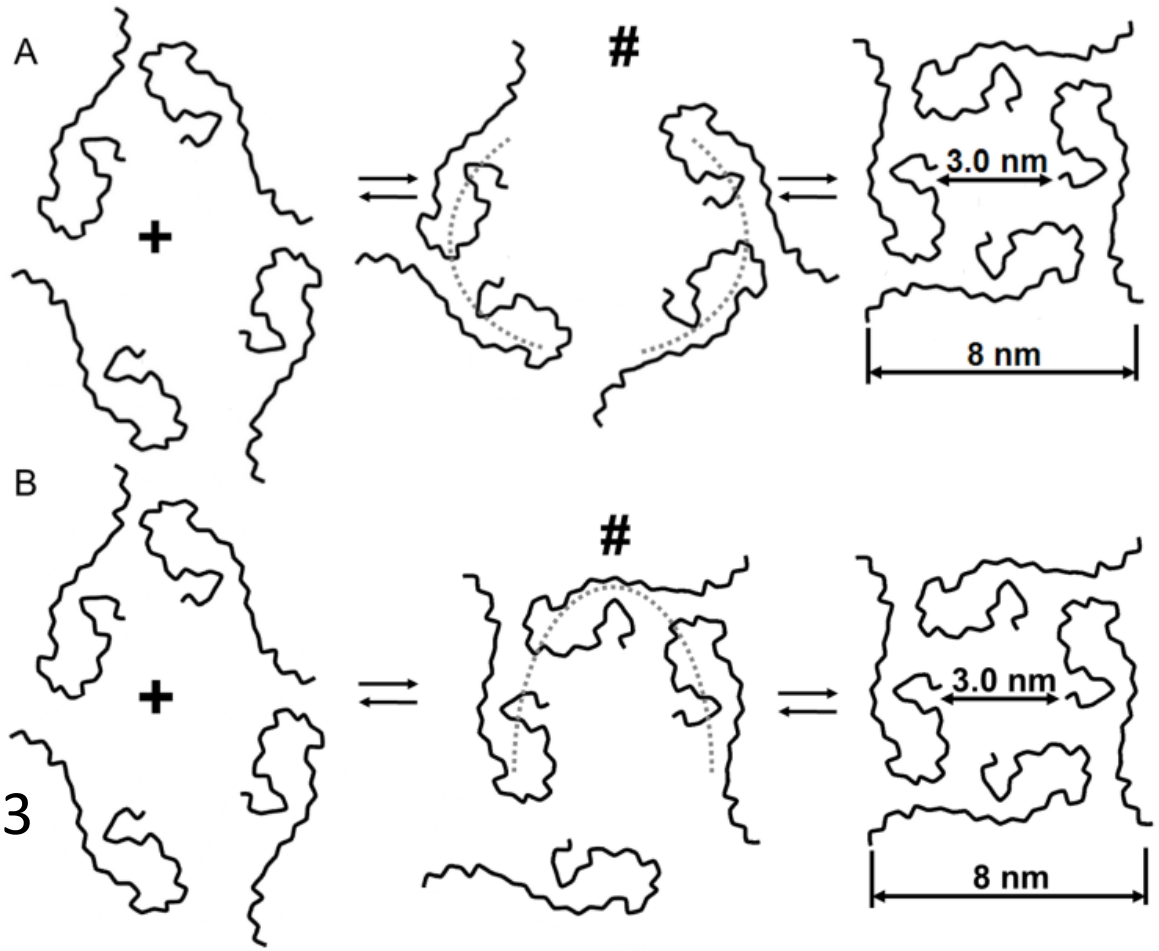

Aβ40, n1=2

Aβ42, , n1=3

Dovidchenko et al., J Struct Biol. 2016 Jun;194(3):404-14.

A. Einstein: "**Only the theory decides what we will manage to watch!**"

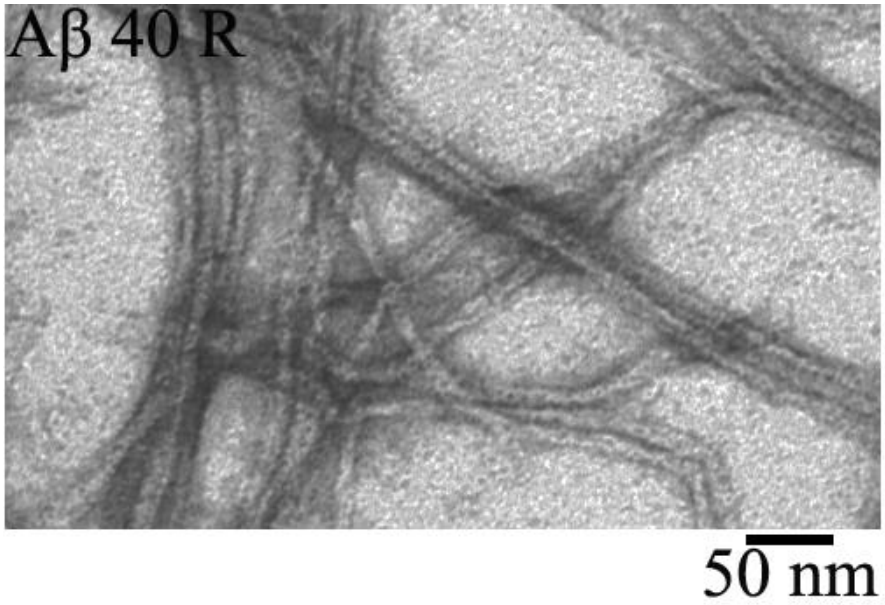

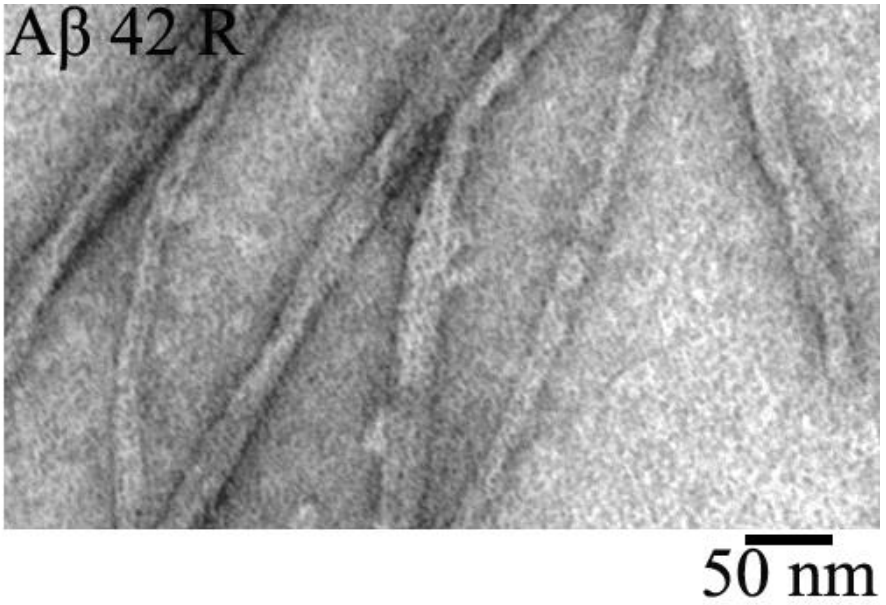

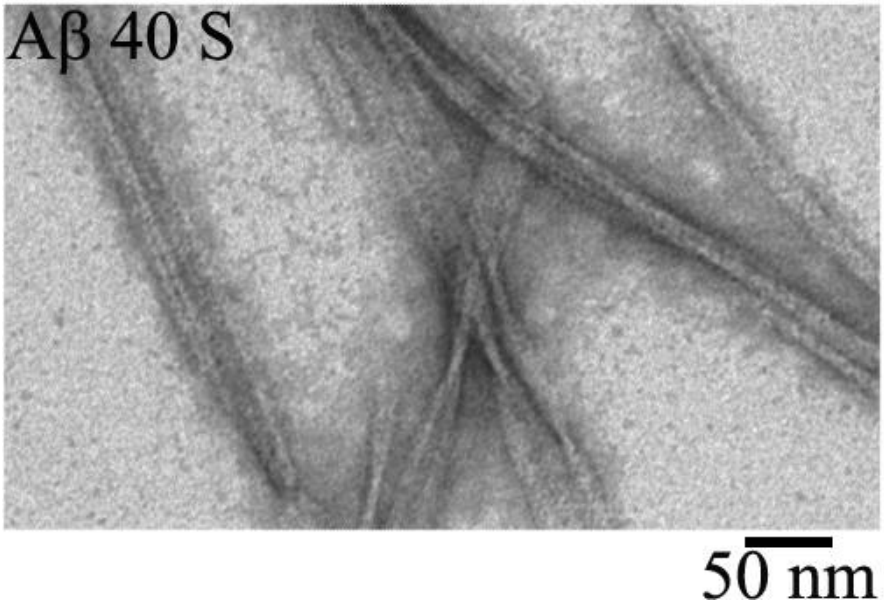

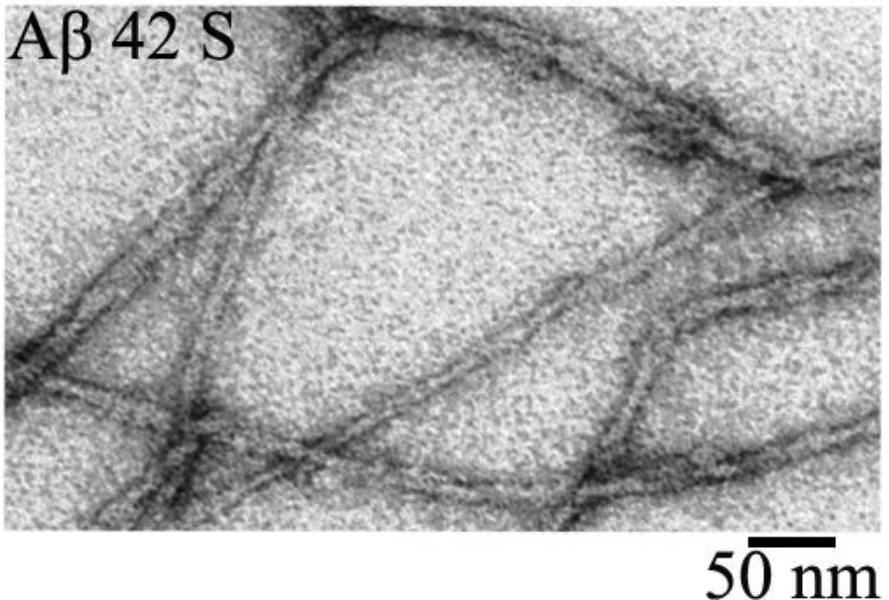

Our model suggests that the generation of fibrils takes place along the following simplified pathway: a monomer – a ring-like oligomer - a mature fibril consisting of ring-like oligomers

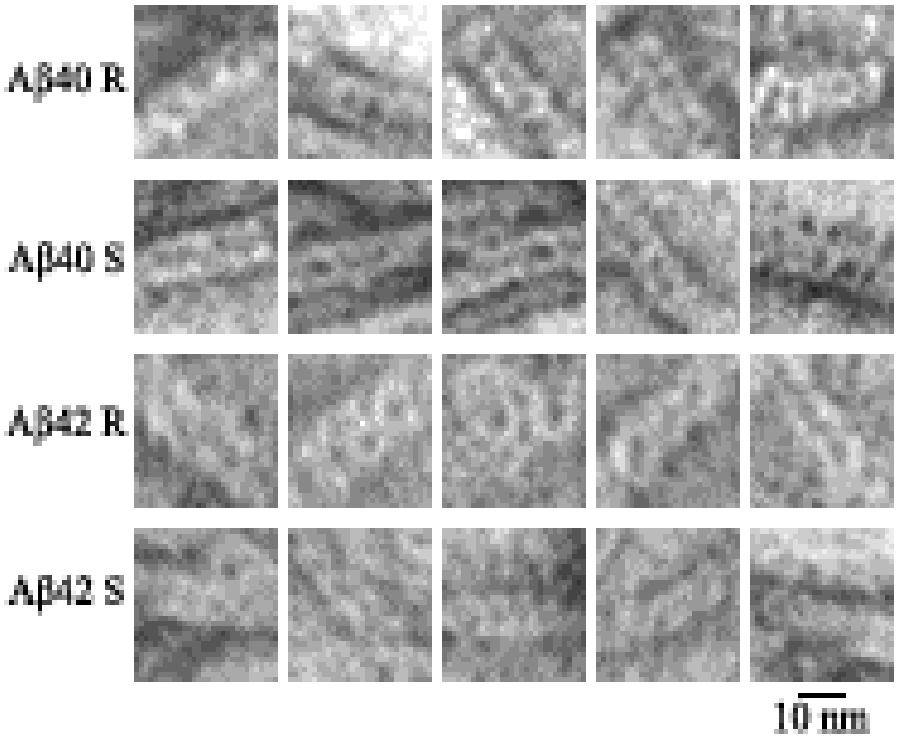

Ring-like structures have a diameter of about 8-9 nm, an oligomer height of about 2-4 nm, and an internal diameter of the ring of about 3 nm.

Selivanova et al., J. of Alzheimer's disease, 2016, 54, 821-830

Our model suggests that the generation of fibrils takes place along the following simplified pathway: a monomer - a ring oligomer - a mature fibril consisting of ring oligomers

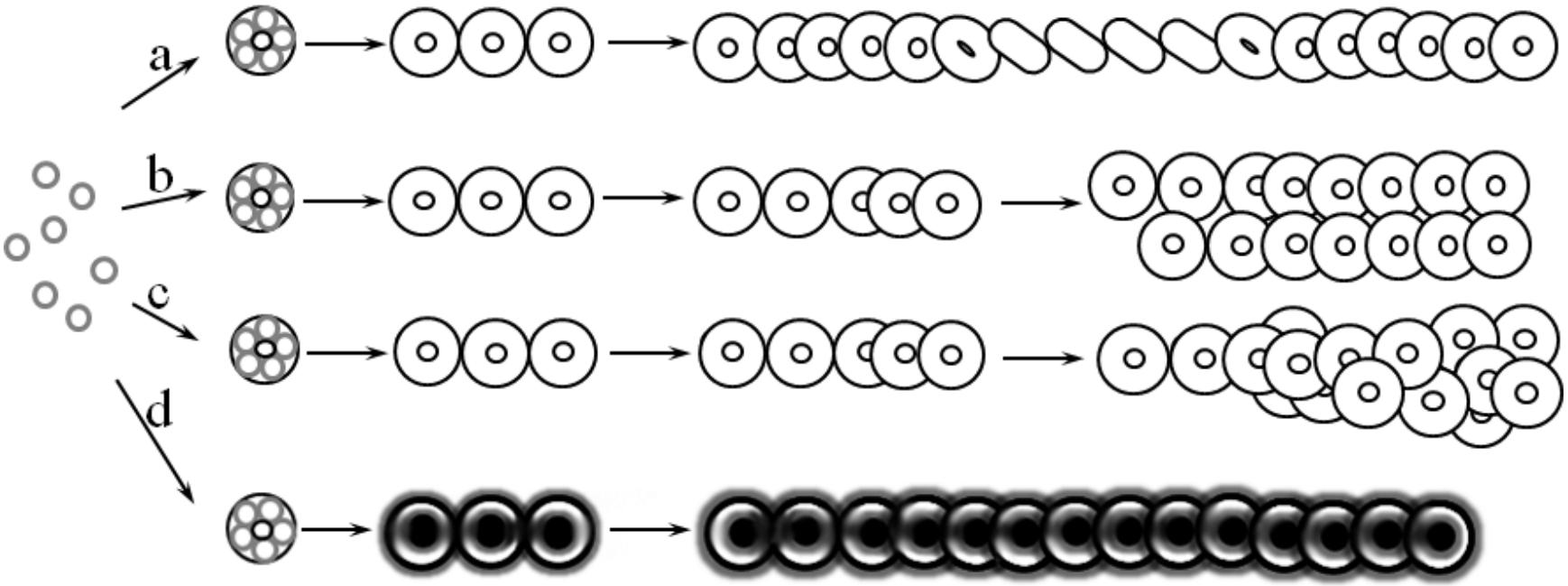

Selivanova et al., J. of Alzheimer's disease, 2016, 54, 821-830

AMYLOID, III. A PROTEIN RELATED TO THE SUBUNIT STRUCTURE OF HUMAN AMYLOID FIBRILS* BY EARL P. BENDITTt AND NILS ERIKSEN

PNAS, 1966, 00141-0082

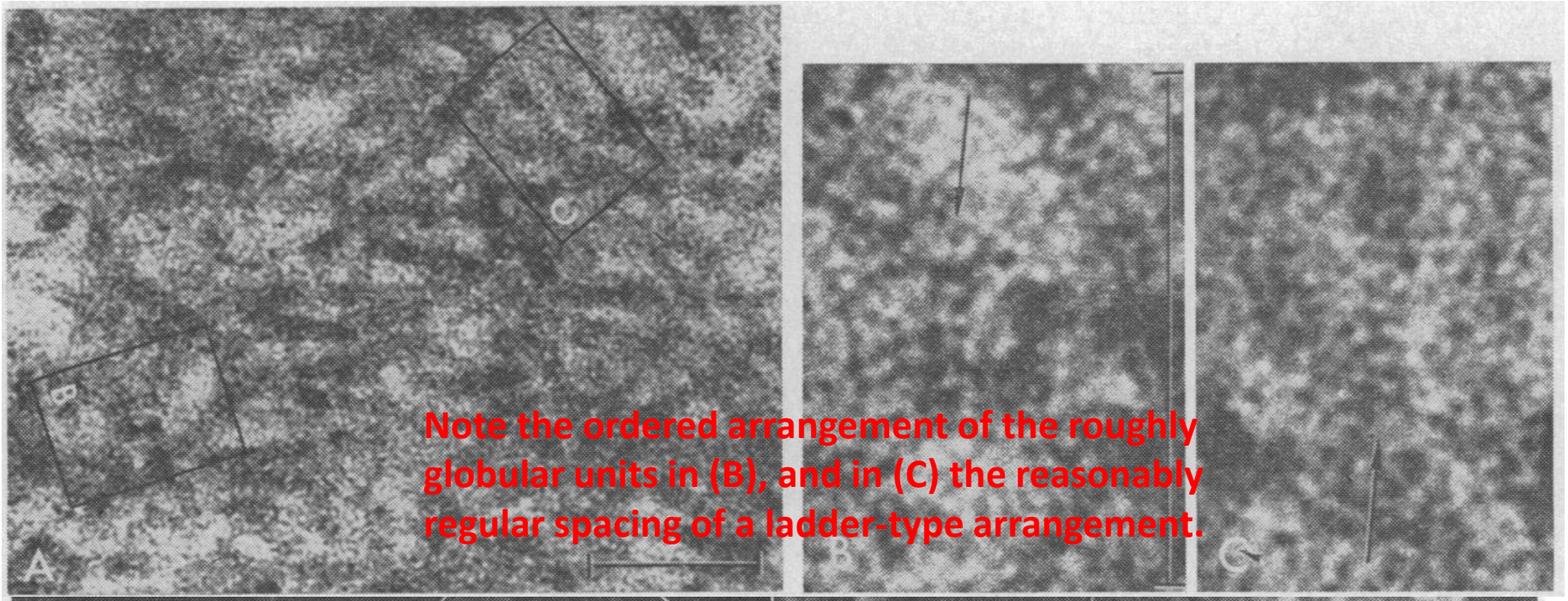

Note the ordered arrangement of the roughly globular units in (B), and in (C) the reasonably regular spacing of a ladder-type arrangement.

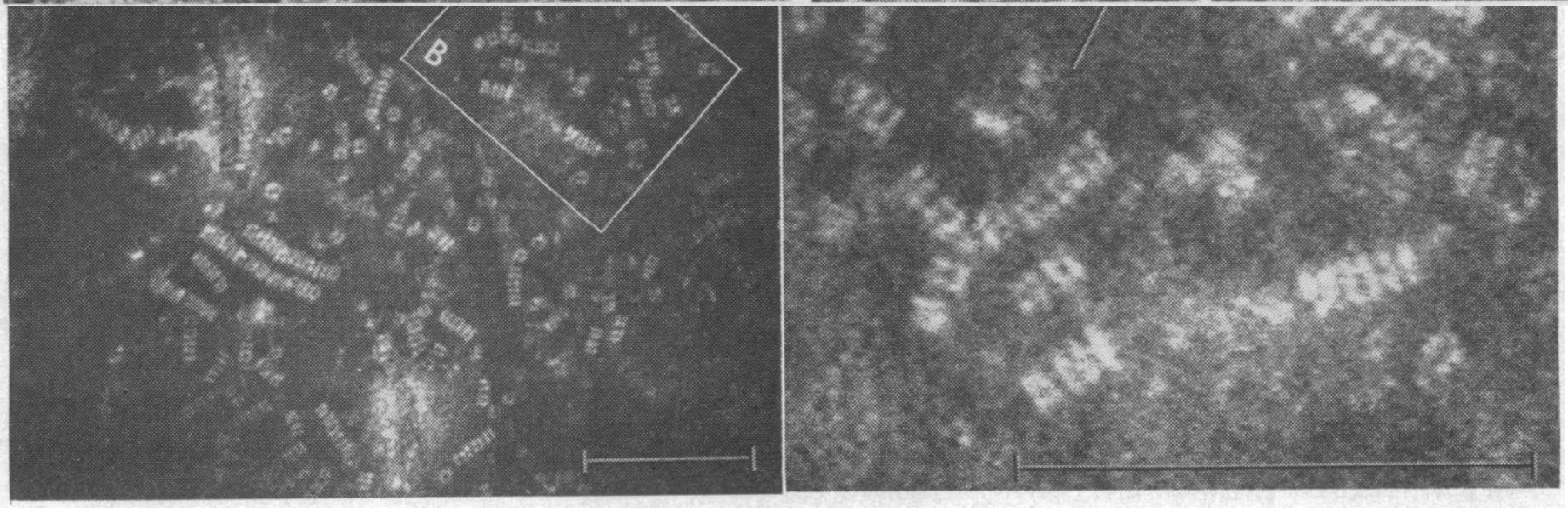

Glenner, et al., J. Histochem. and Cytochem. ,1968, 16, 633–644.

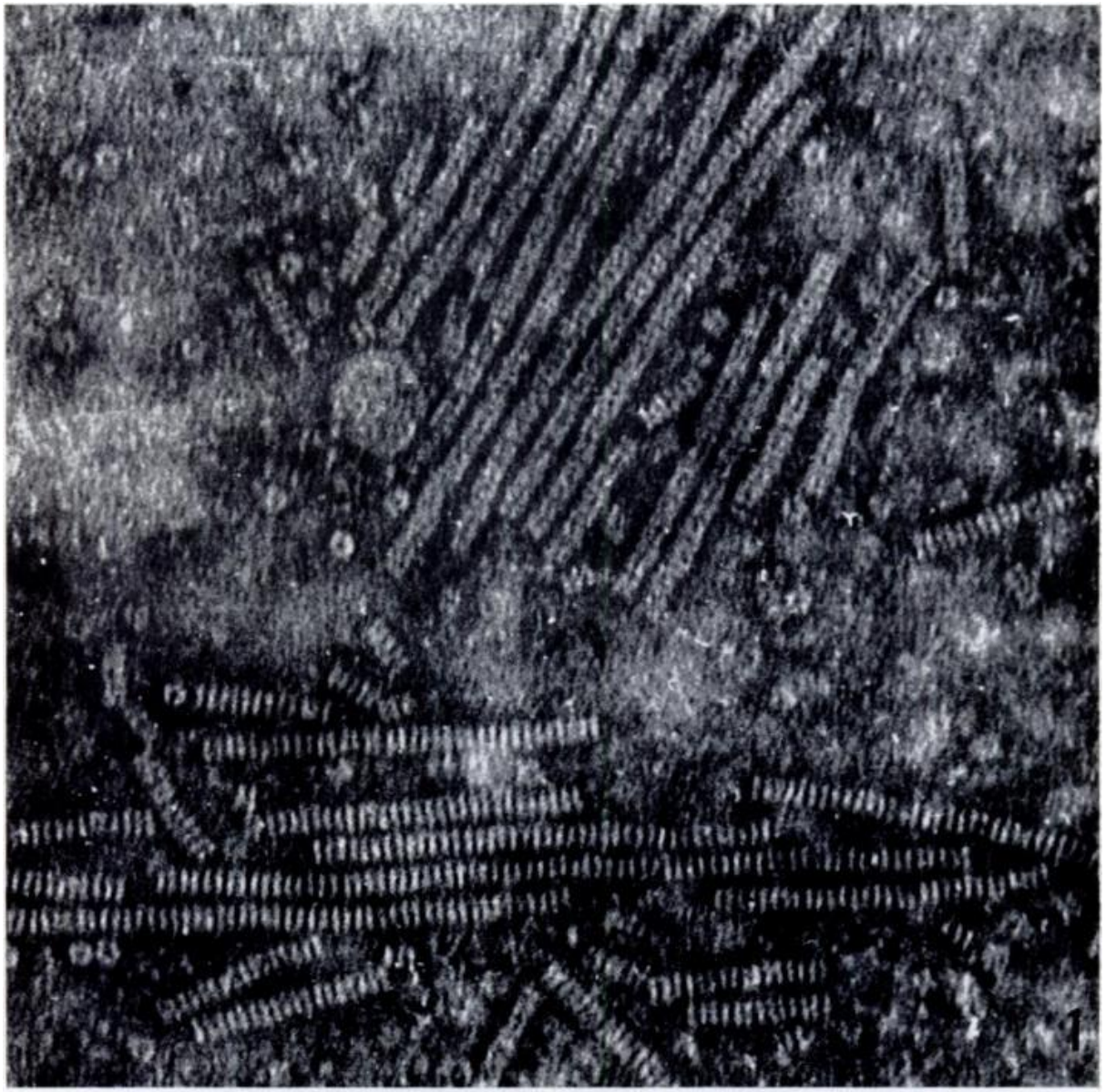

A negative stained preparation from amyloidotic human spleen demonstrating long periodic rods, (composed of stacked pentagonal unit structures or “doughnuts”) up to 2,500A in length, and a small unit structures, approximately 90A in diameter.

DETERMINATION OF REGIONS INVOLVED IN AMYLOID FIBRIL FORMATION FOR Aβ40 and Aβ42 PEPTIDES

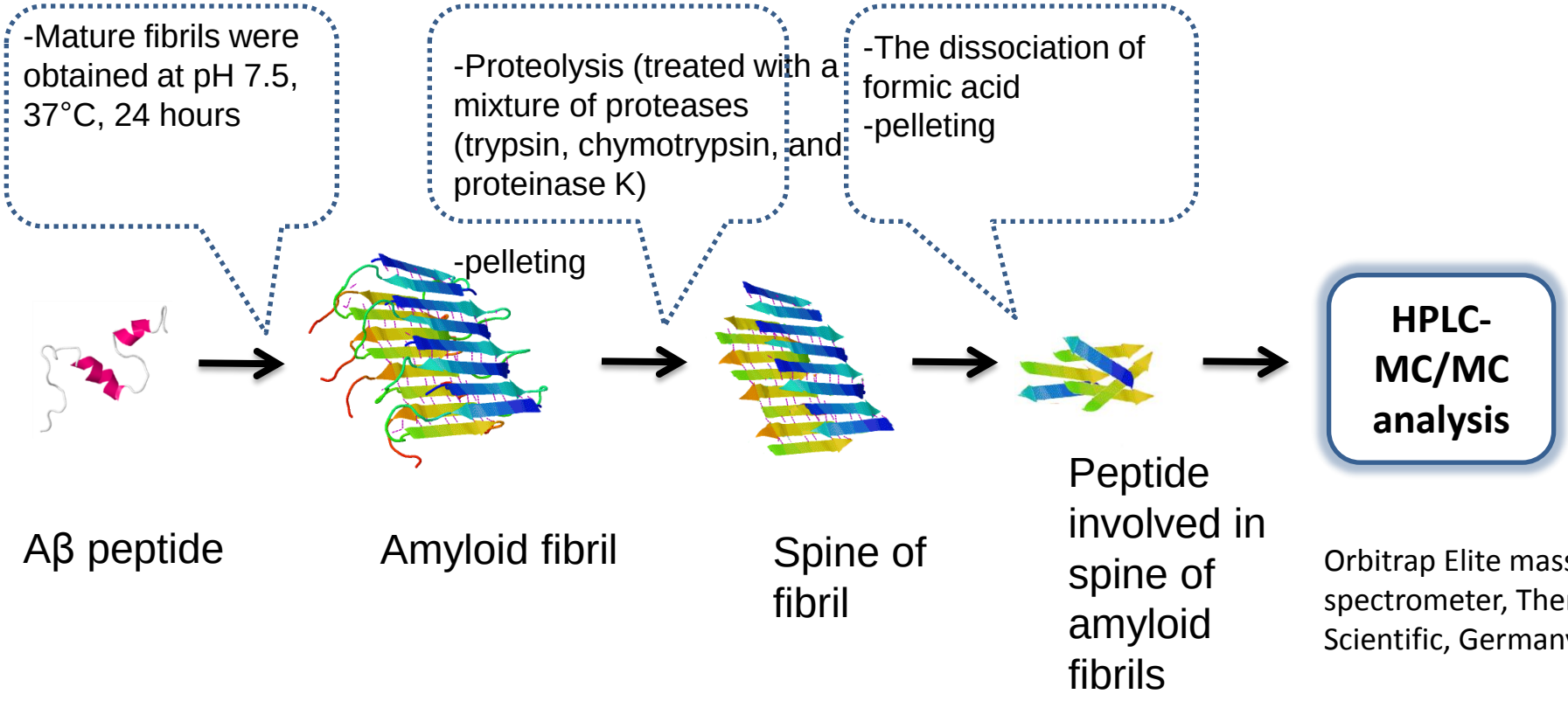

Amyloidogenic peptides were separated using the liquid chromatography / tandem MS technique, and identified by PEAKS Studio 7.5 program. This program makes it possible not only to identify peptides but also to estimate their relative concentration in the probe.

Peptides detected after proteases treatment of amyloid fibrils formed by Aβ40 and Aβ42

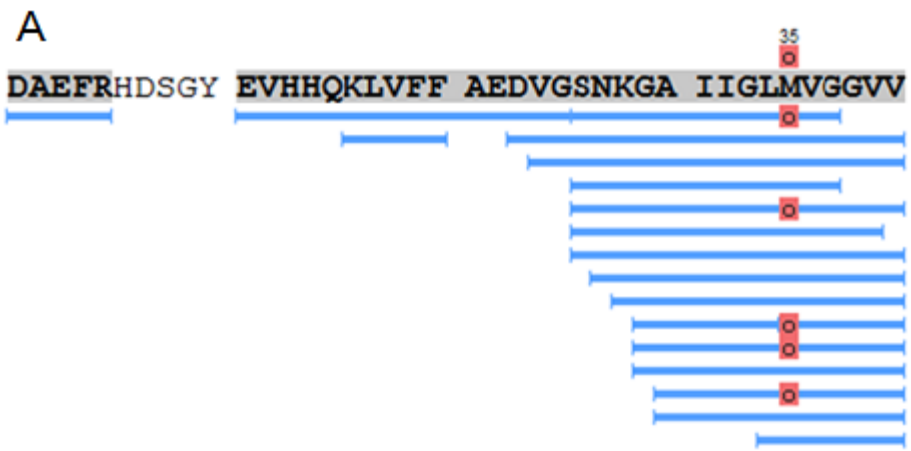

The obtained data showed that protease-resistant regions were the ones from 16 to 20 and from 26 to 40 amino acid residues in Aβ40 peptide molecule, whereas a more complicated distribution of protected regions of the chain is observed for Aβ42.

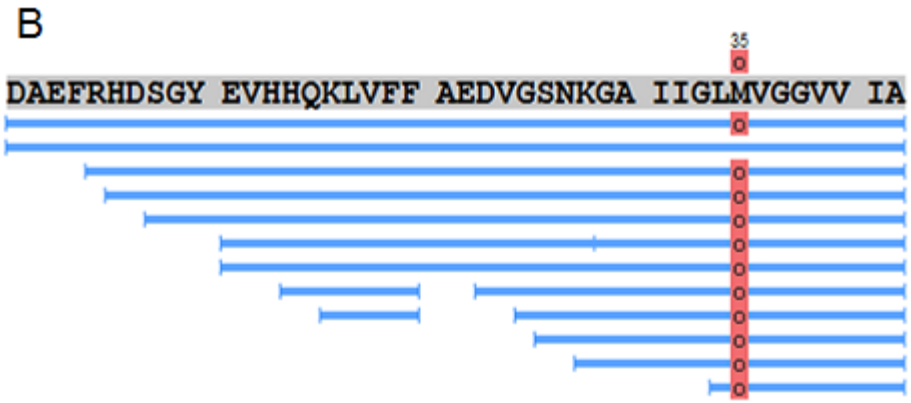

In some molecules, the region from 26 to 42 amino acid residues is protected, but in other molecules only several N-terminal amino acid residues are excised, and the remaining part is inaccessible to proteases. These data agree with the EM data showing that the diameter of the recombinant Aβ42 fibrils varies much greater (8-35 nm) as compared to that of Aβ40 (8-9 nm).

Surin et al., Biochemistry (Moscow), 2016; Selivanova et al., J. Alzheimer Dis., 2016, 54

A. Einstein: "**Only the theory decides what we will manage to watch!**"

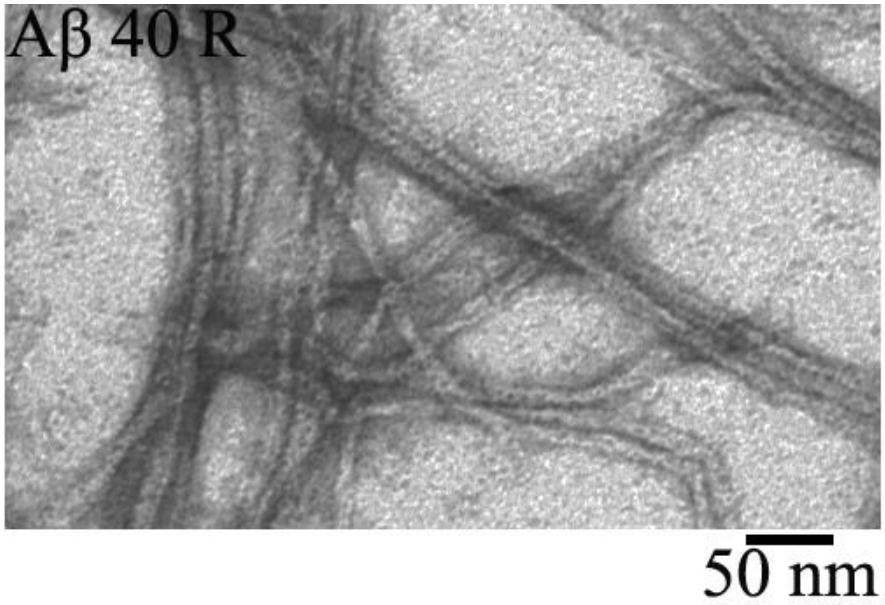

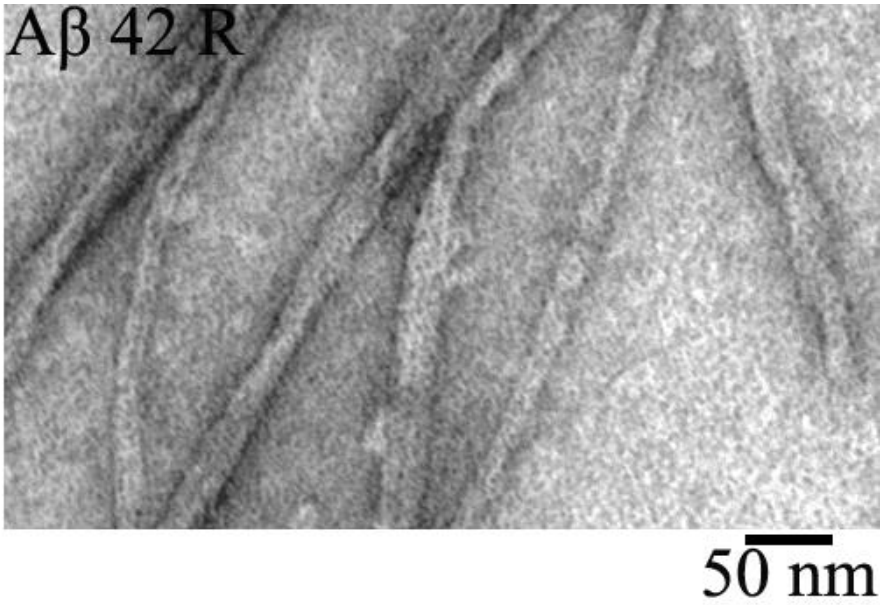

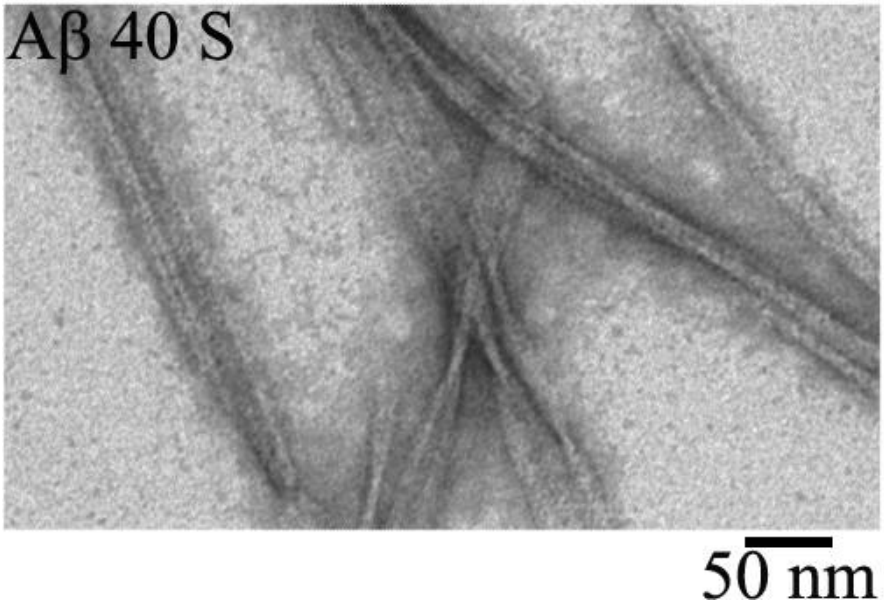

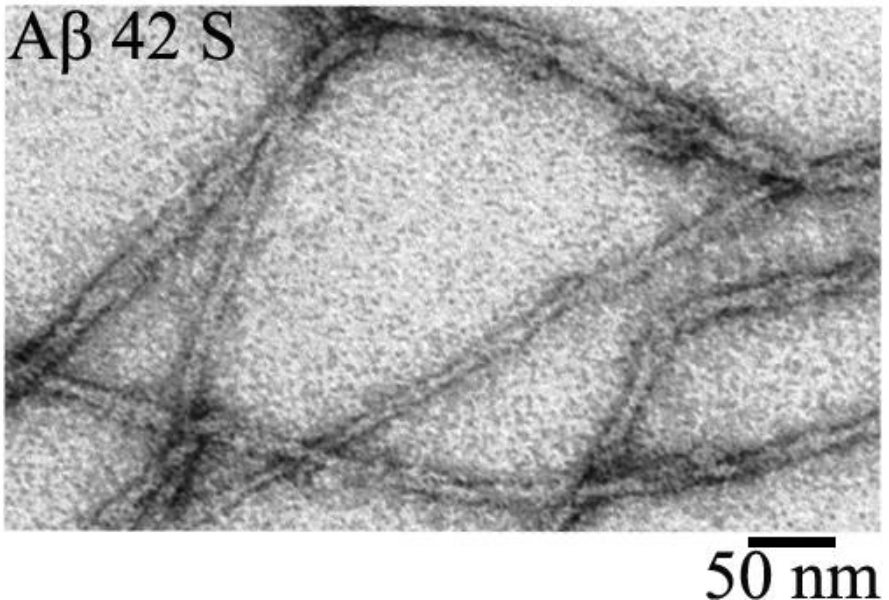

Characteristics of cross-beta structure

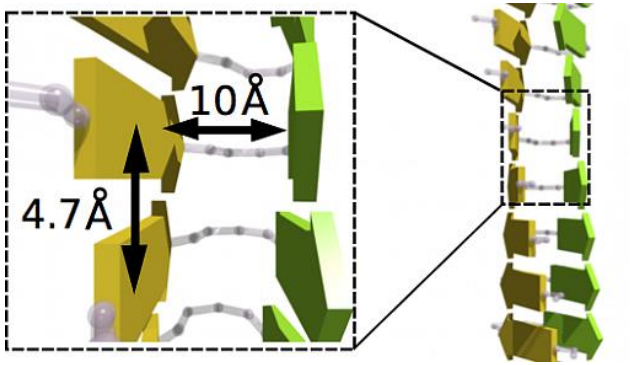

Scheme of cross-β structure, изображающая упаковку параллельных β-тяжей перпендикулярно оси фибриллы

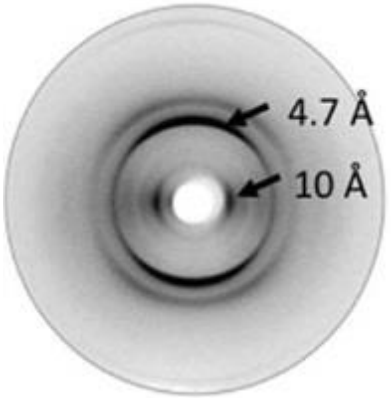

Diffraction picture от amyloid fibrils, [Serpell, 2014].

Полученные нами данные для Aβ-пептида:

Fibril morphology

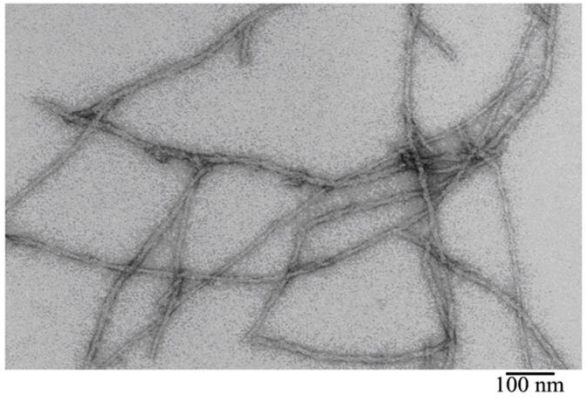

Characteristic reflections

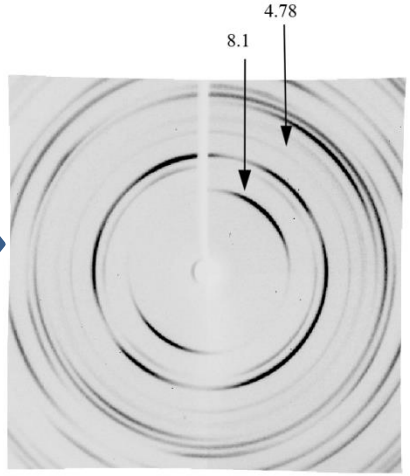

These aggregates are amyloid fibrils

Comparison of X-ray diffraction patterns of amyloid fibrils of synthetic (Sigma) preparations Aβ40 and Aβ42 (concentrated from 0.05 M Tris-HCl, pH 7.5) and the preparation of 0.5 M Tris-HCl (pH 7.5).

Aβ40 peptide

Aβ42 peptide

0.5 M Tris-HCl (pH 7.5), absent only reflections 4.4, 4.8,6.3

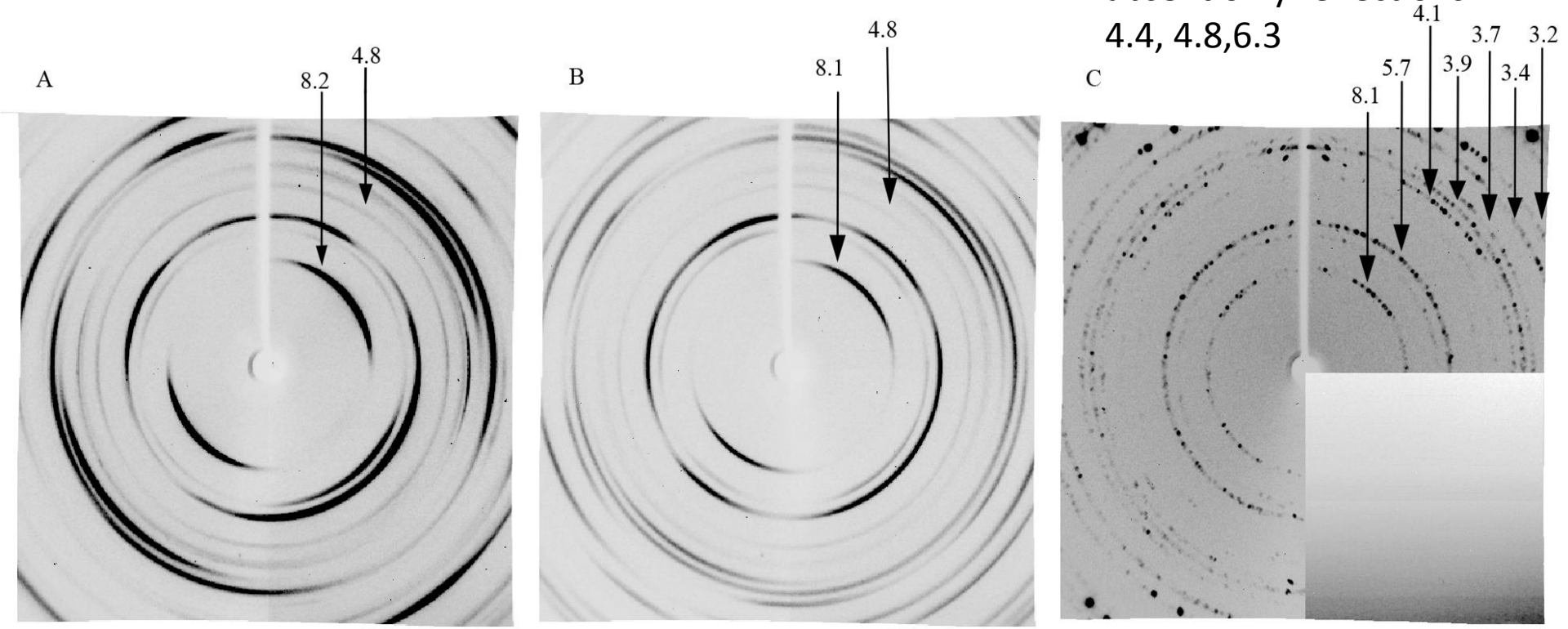

A three dimensional model of amyloid fibrils for Aβ40 and Aβ42 peptides

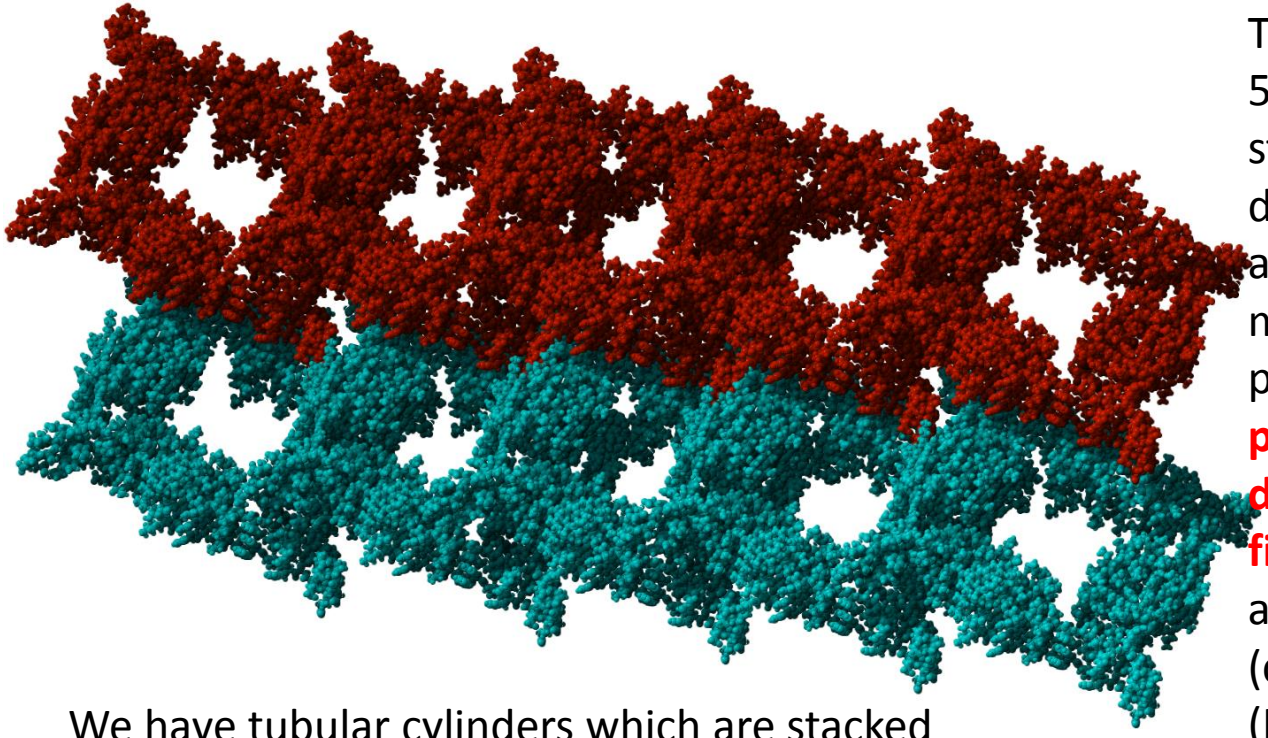

We have tubular cylinders which are stacked with a 53 Å period, which corresponds to our model distance.

Selivanova et al., J. of Alzheimer's disease, 2016, 54, 821-830

The meridional reflection at 53 Å indicates a periodic structure along the H-bonding direction. Models that could account for the low-angle meridional reflections in Aβ peptides 9-28 and 1-40 are (a) **periodic arrangement of discrete objects along the fibril axis**, (b) staggered arrangement of subfibrils, and (c) twisting of the fibril (Inouye et al., Biophys.J. 1993). Case (a) supports our model both for Aβ40 and for the short peptide of 10 residues long.

PDB entry 2M4J was used for modeling. Arg5-Glu22 inter- and Asp23-Lys28 intra-peptide salt bridges present in the dodecamer structure, which is the building block of fibrils. Oligomers overlap in the same row and between the rows.

Malinchik et al., Biophys.J. 1998, 74, 537-545

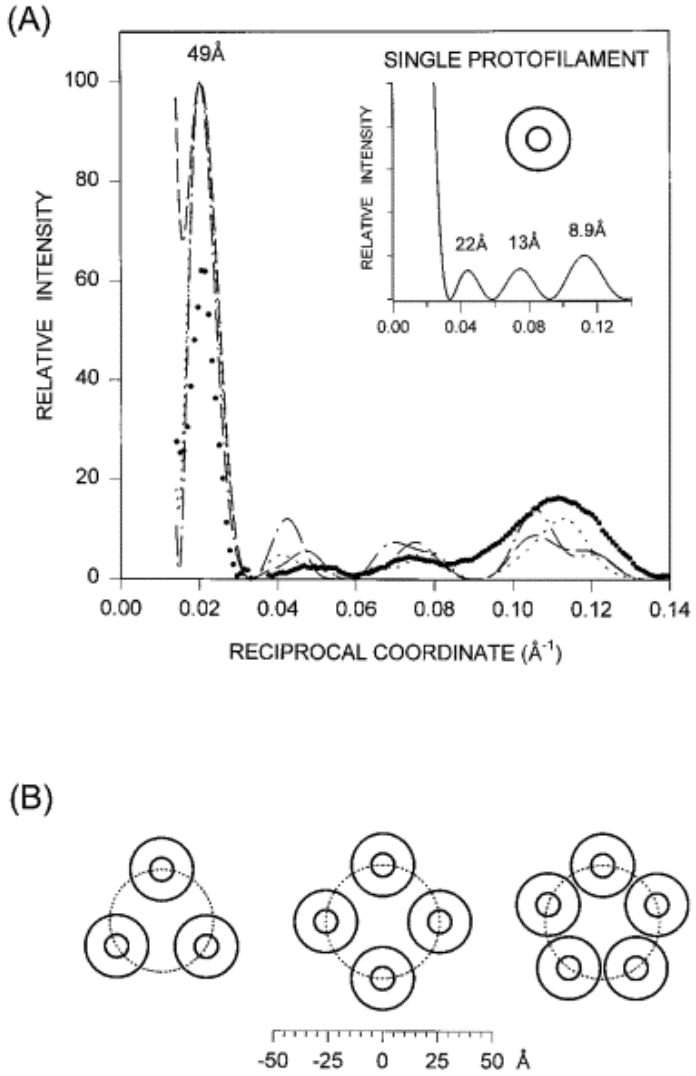

Modeling of the equatorial x-ray diffraction data from A*β*(1–40). (*A*) Experimental and calculated equatorial intensities for single (*A*, *inset*) and multiple (*B*) tubular protofilaments. For the latter, the protofilaments were arranged on the circumference of a circle whose radius was consistent with the first interference peak at 49.2 Å (see text for details). To reveal the low-angle region at ~0.02 $Å^{-1}$, densitometer traces of the first and second films were scaled and combined. The background was subtracted as described in Materials and Methods. Points (●), Experimental data; — —, three protofilaments; – – –, four protofilaments; — - —, five protofilaments.

The separation of the objects is within the range 55-57A. This is smaller than the 70A fiber size observed by electron miscroscopy.

When calculated with *r*1 14.3 Å and *r*2 5.3 Å, this model gives three broad equatorial reflections at spacings of 22, 13, and 8.9 Å, as shown in Fig. 6.

Taking into account such molecular mechanism of Aβ40 and Aβ42 amyloid formation it is easier to explain such process as:

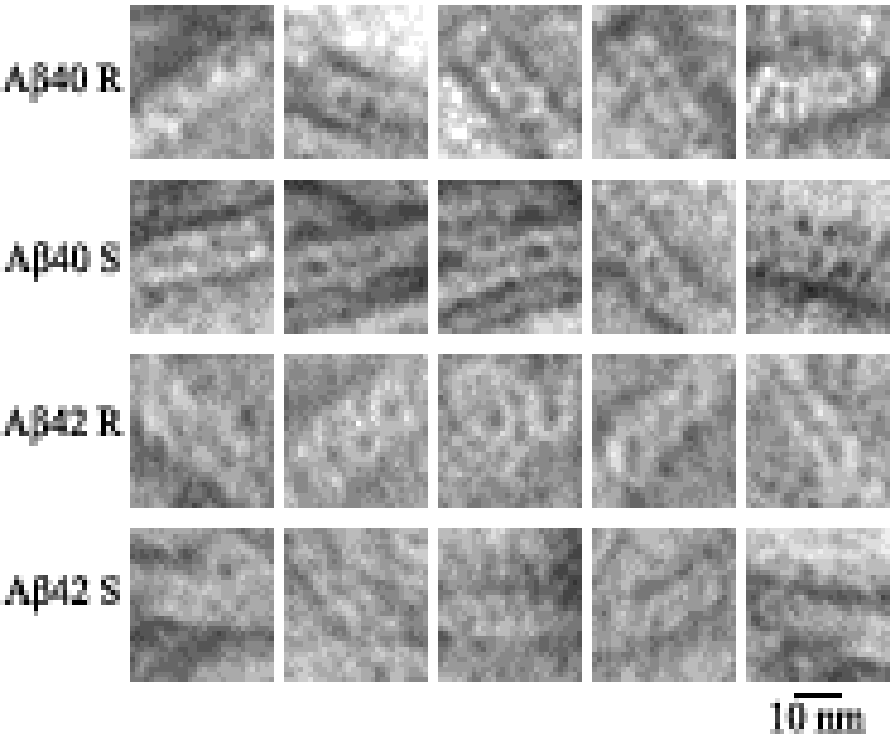

1) different polymorphism (different laboratories are studying different polymorphs),
2) affinity of specific antibodies to protofibrils and oligomers ,
3) discrepancies between H/D exchange and solid state NMR,
4) small fluorescence intensity of thioflavin T,

5) fragmentation, spontaneous fibril breaking and rejoining ,
6) dodecamer is the terminal species observed in the Ion Mobility-MS experiments , and
7) the presence of water in the holes of ring-like oligomers .

Mechanism of fatty acid-derived oligomers (LFAO)Propagation

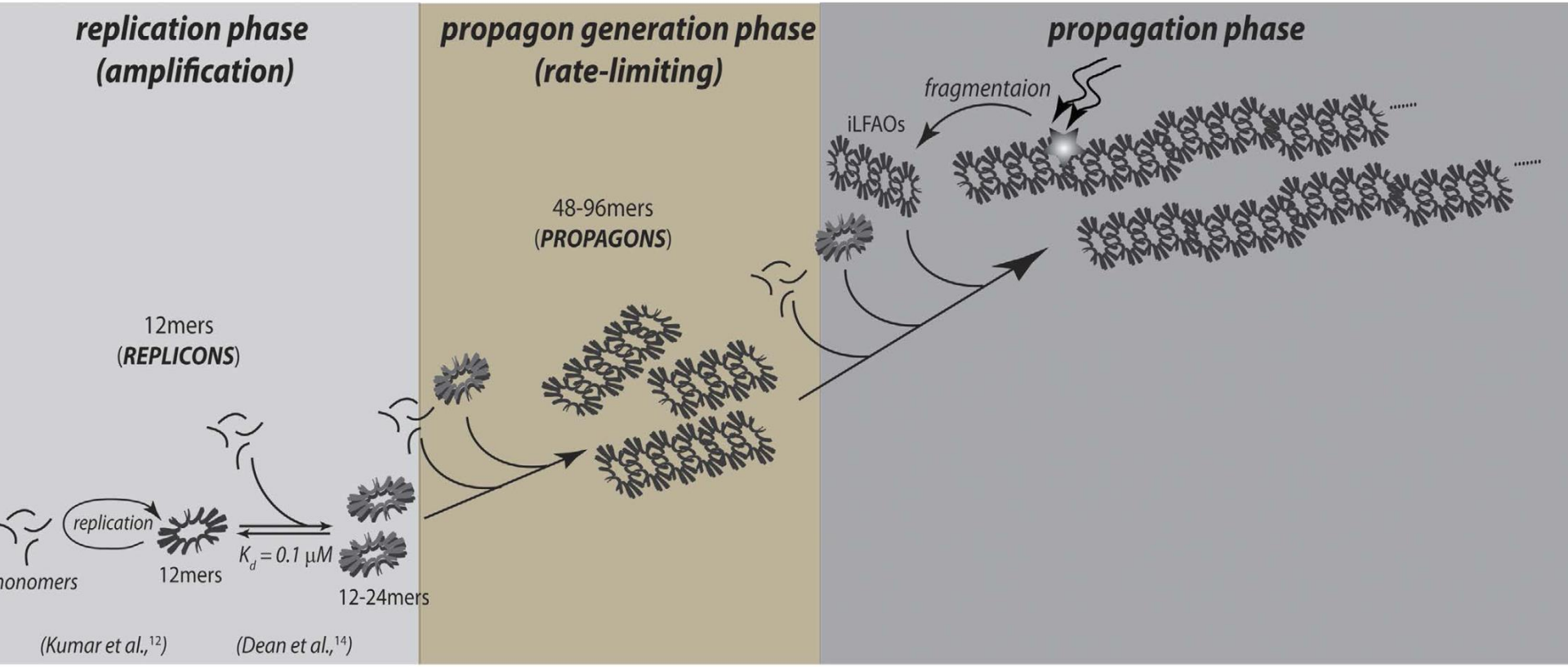

Scientific **Reports** | 7:40787 | DOI: 10.1038/srep40787

Schematic representation of the possible mechanism of fibril formation by the fragments of Aβ peptide

1, 2 – Aβ(31-40) (ribbons and bundles, respectively)

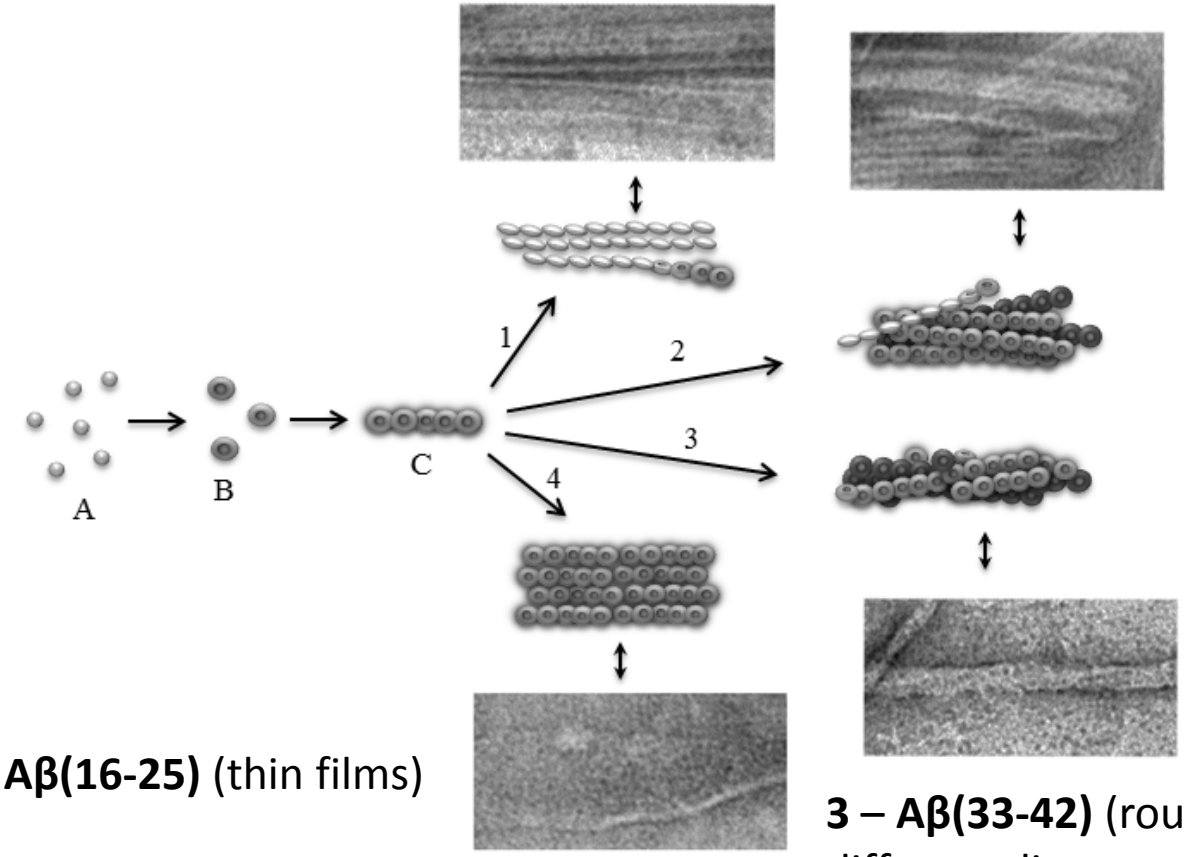

4 – Aβ(16-25) (thin films)

3 – Aβ(33-42) (rough bundles with different diameters)

Formation of fibrils of insulin molecules occurs via and by means of oligomer ring structures: monomer → reorganized hexamer → fibrils → cluster of amyloid fibrils

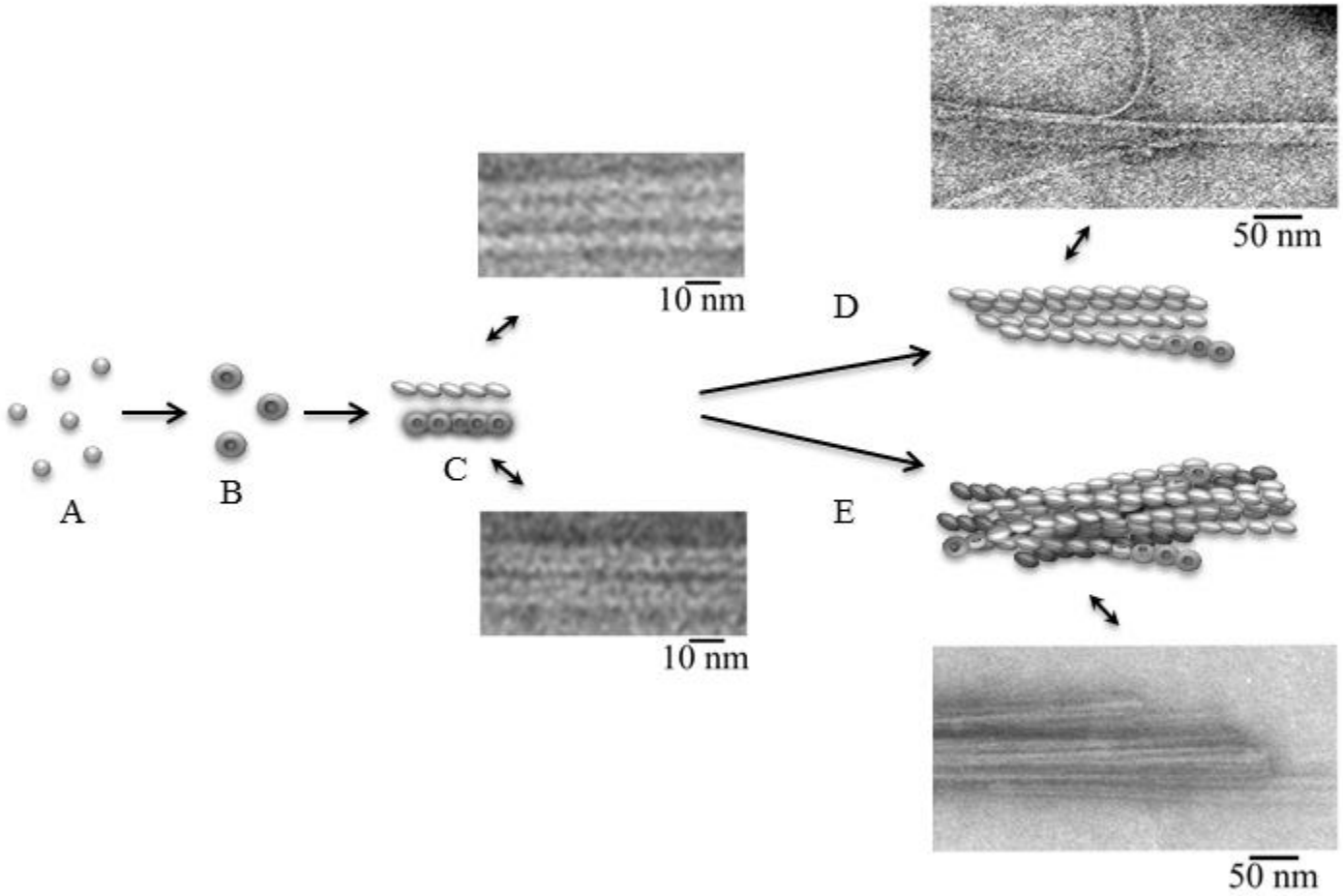

Selivanova et al., Curr Protein Pept Sci. 2017, 18, 57-64.

Conclusion

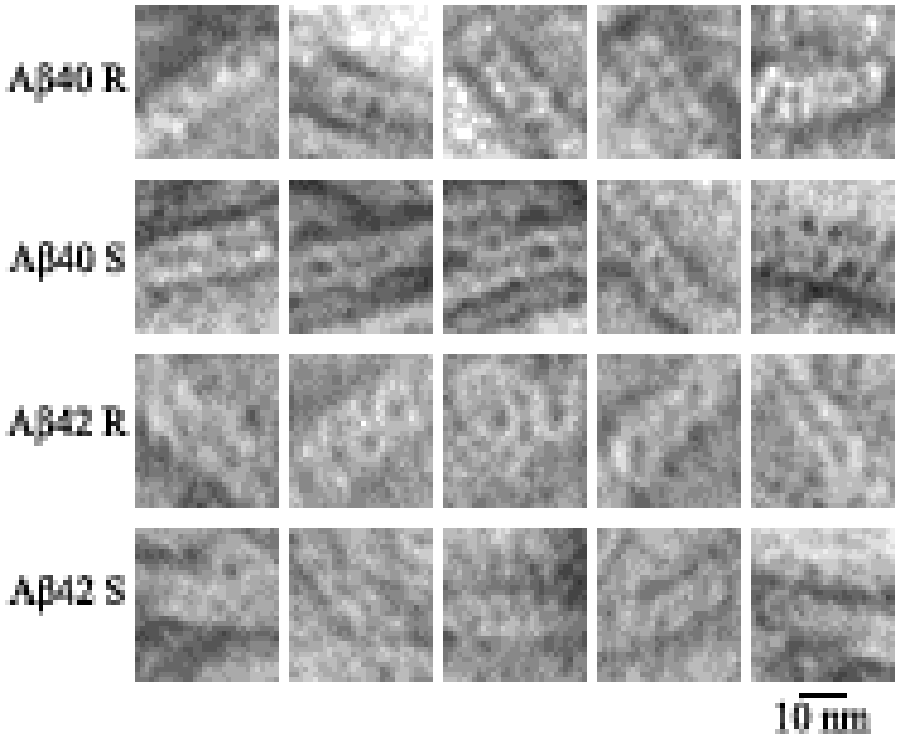

1) The combination of our theoretical and experimental results allowed us to propose a new model of structural organization of an amyloid fibril. Our model suggests that the generation of fibrils takes place along the following simplified pathway: a monomer - a ring oligomer - a mature fibril consisting of ring oligomers.

2) We have demonstrated that oligomers act as a growing unit for the fibril formation (**Aβ, insulin, fragments of Bgl2p and Aβ)** and nanofilm formation (fragment **Aβ(16-25)**).

Нужно ли применять персонифицированный подход к лечению амилоидозов?

- В литературе встречается мнение, что при разработке терапевтических средств против амилоидозов следует применять персонифицированный подход, поскольку показано, что фибриллярные образования у разных пациентов могут морфологически различаться. В этой связи обнаружение нами единого для всех фибрилл способа формирования фибрилл из олигомерных структур могло бы облегчить создание препаратов общего действия. Однако, на наш взгляд, основное внимание должно быть уделено не полимерным образованиям белков/пептидов в виде фибрилл и даже не олигомерным агрегатам, а физиологическим, генетическим и другим причинам, приводящим к дестабилизации нативных молекул белков/пептидов и запускающим процесс формирования фибрилл.

Thank you for your attention!

N.V. Dovidchenko, O. M. Selivanova, M. Yu. Suvorina, E.I. Grigorashvili, V.V. Marchenkov, U.F. Dzhus, A. K. Surin, A.O. Michailina, N.D. Nikulin

This study was supported by the Russian Science Foundation

Kinetic scenario 3: Exponential growth: Fibril ends multiplication by branching

leads to a **large** relative duration L_{rel} of the lag-period

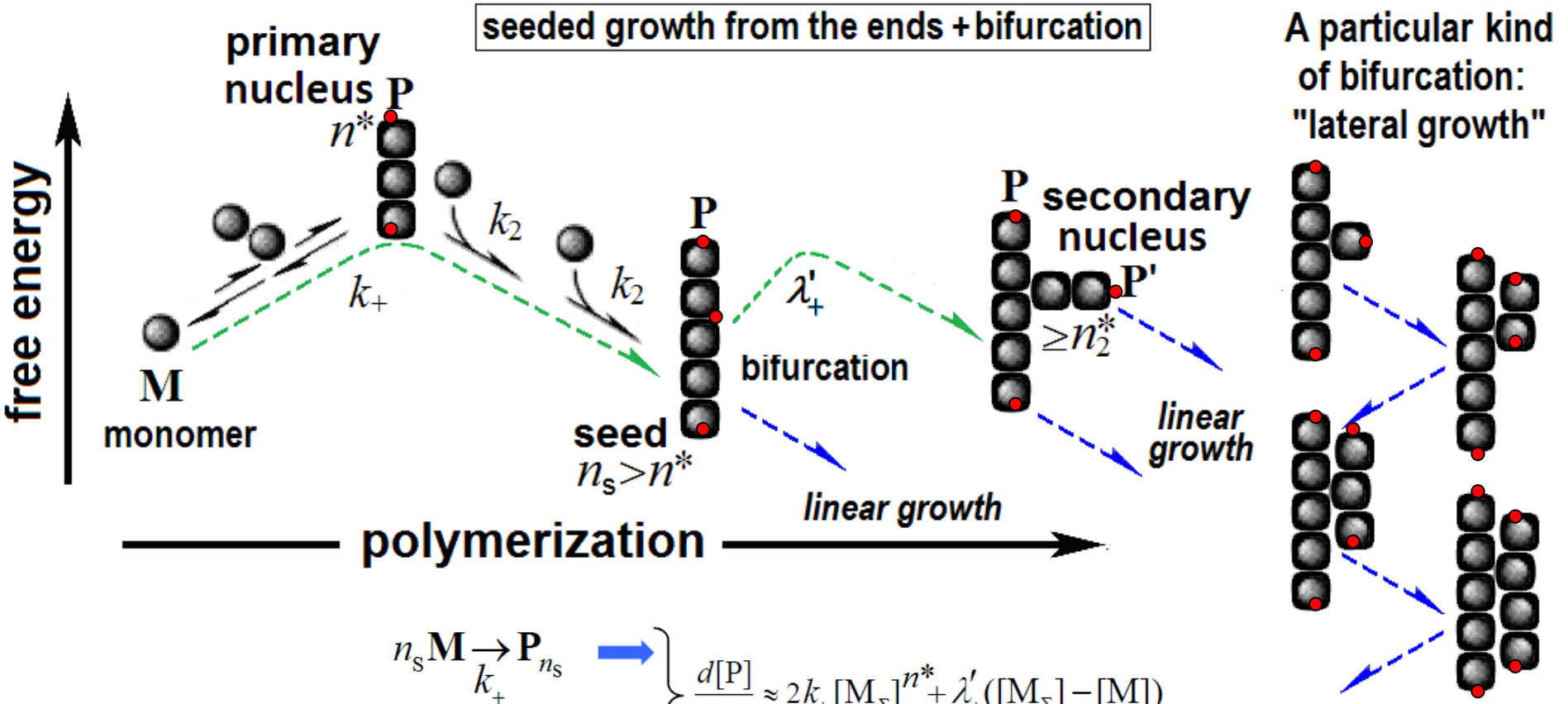

$$n_s \mathbf{M} \xrightarrow[k_+]{} \mathbf{P}_{n_s}$$

$$\mathbf{P} \xrightarrow[\text{all\_fibr.}\times\lambda'_+]{} \mathbf{P}, \mathbf{P}'$$

$$\frac{d[\mathrm{P}]}{dt} \approx 2k_+[\mathrm{M}_\Sigma]^{n^*} + \lambda'_+([\mathrm{M}_\Sigma]-[\mathrm{M}])$$

$$\mathbf{P}_n + \mathbf{M} \xrightarrow[\text{all\_ends}\times k_2]{} \mathbf{P}_{n+1} \qquad \frac{d[\mathrm{M}]}{dt} \approx -k_2[\mathrm{P}][\mathrm{M}_\Sigma]$$

→ approx. **analytical** solution for early stages of the process